

BGD

10, 2889–2936, 2013

**Seasonal cycle of
biogenic flux in the
equatorial Indian
Ocean**

P. J. Vidya et al.

Influence of physical and biological processes on the seasonal cycle of biogenic flux in the equatorial Indian Ocean

P. J. Vidya¹, S. Prasanna Kumar¹, M. Gauns¹, A. Verenkar¹, D. Unger², and V. Ramaswamy¹

¹National Institute of Oceanography, Dona Paula, Goa-403 004, India

²Leibniz Centre for Tropical Marine Ecology GmbH, Fahrenheitstraße 6, 28359 Bremen, Germany

Received: 13 December 2012 – Accepted: 19 December 2012 – Published: 18 February 2013

Correspondence to: S. Prasanna Kumar (prasanna@nio.org)

Published by Copernicus Publications on behalf of the European Geosciences Union.

Title Page

Abstract

Introduction

Conclusions

References

Tables

Figures

⏪

⏩

◀

▶

Back

Close

Full Screen / Esc

Printer-friendly Version

Interactive Discussion

Abstract

Seasonal cycle of biogenic fluxes obtained from sediment trap at two locations 5° 24' N, 86° 46' E (SBBT) and 3° 34' N, 77° 46' E (EIOT) within the equatorial Indian Ocean (EIO) were examined to understand the factors that control them. The sediment trap data at SBBT were collected for ten years from November 1987 while that at EIOT was for one year period from January 1996. The characteristic of biogenic flux at SBBT was the strong seasonality with peak flux in August, while lack of seasonality characterized the flux at EIOT. At the SBBT and EIOT, the higher chlorophyll biomass during summer monsoon was supported by wind-mixing, which supplied new nitrogen to the upper ocean. The stronger winds at SBBT compared to EIOT resulted in greater entrainment of nutrients to the euphotic zone, which supported higher chlorophyll biomass. High cell counts of phytoplankton (> 5 µm) at SBBT dominated by diatoms suggest the operation of classical food web and high carbon export. On the contrary, one-and-half time higher magnitude of micro-zooplankton biomass dominated by picophytoplankton along with 2-fold lesser meso-zooplankton at EIOT indicated the importance of microbial loop. The substantial decrease in the carbon export at EIOT indicated faster remineralization of photosynthetically produced organic matter. We see a striking similarity between the biological process that operates in the SBBT with that of the equatorial Atlantic and EIOT with that of the equatorial Pacific, though the physical forcing in these three regions, namely EIO, the equatorial Atlantic and the equatorial Pacific, are very different.

1 Introduction

Equatorial regions are special areas of the world ocean where intense air-sea interaction occurs. The tight coupling between the ocean and atmosphere makes this region sensitive and hence important for earth's climate. The global carbon cycle plays an important role in earth's climate and primary production forms an integral part of it. Studies of primary production often use chlorophyll as an estimator of phytoplankton

BGD

10, 2889–2936, 2013

Seasonal cycle of biogenic flux in the equatorial Indian Ocean

P. J. Vidya et al.

Title Page

Abstract

Introduction

Conclusions

References

Tables

Figures

⏪

⏩

◀

▶

Back

Close

Full Screen / Esc

Printer-friendly Version

Interactive Discussion

BGD

10, 2889–2936, 2013

**Seasonal cycle of
biogenic flux in the
equatorial Indian
Ocean**

P. J. Vidya et al.

[Title Page](#)[Abstract](#)[Introduction](#)[Conclusions](#)[References](#)[Tables](#)[Figures](#)[⏪](#)[⏩](#)[◀](#)[▶](#)[Back](#)[Close](#)[Full Screen / Esc](#)[Printer-friendly Version](#)[Interactive Discussion](#)

biomass (Harris, 1986). Phytoplankton produces half of the oxygen we breathe, draw down the atmospheric CO₂, and ultimately controls the global climate system (Siegel and Franz, 2010). In the ocean, productivity is controlled by the availability of nutrients and sunlight. Productivity signal can be transferred rapidly to the deep sea by settling particles from the surface (Asper et al., 1992). The biological pump in the upper ocean transfers biogenic compounds from the surface into deep waters in the form of particulate organic matter (Bishop, 1989; Longhurst, 1995; Ittekkot, 1993). Each year, the biological pump removes 7.9–13.1 GT C (1 GT = 10¹⁵ g) of the estimated 40–60 GT C produced in the surface ocean (compiled in Boyd and Trull, 2007; Carr et al., 2006). Between region and events, the export fraction may vary between 2–20 % (Buesseler, 1998). The fraction of primary production which is exported to waters deeper than 1500 m is also highly variable and ranges between 0.1–8.8 % (Lutz et al., 2002). In the equatorial Pacific, physical as well as biological processes such as upwelling and remineralization by smaller organisms make it a large source of CO₂ to the atmosphere (Murray et al., 1994). This remineralization in turn leads to less export of carbon to ocean interior in the equatorial Pacific (Beatriz et al., 2001). In contrast, strong upwelling and the dominance of faster-sinking diatoms (Bradtmitter et al., 2007) support high export of biogenic flux into the deeper ocean in the equatorial Atlantic. However, we do not have such information in the equatorial Indian Ocean.

The equatorial Indian Ocean (EIO) behaves uniquely compared to the other equatorial regions of the world ocean primarily due to the seasonal reversal of the winds between winter (November–February) and summer (June–September) (Hastenrath and Greishar, 1989). In response to the wind reversals surface currents also reverse in the EIO. During June to September the summer monsoon current (SMC) flows eastward in the EIO, while the winter monsoon current (WMC) flows westward during November to February (Shankar et al., 2002). Between the monsoons, during the spring (April–May) and fall (October–November) transition periods, the consistent westerly winds drive a strong narrow eastward jet known as Wyrтки jet (Wyrтки, 1973) which is equatorially-trapped (Knox, 1976; Gonella et al., 1982; Reverdin and Luyten, 1986). The jet initially

Seasonal cycle of biogenic flux in the equatorial Indian Ocean

P. J. Vidya et al.

[Title Page](#)

[Abstract](#)

[Introduction](#)

[Conclusions](#)

[References](#)

[Tables](#)

[Figures](#)



[Back](#)

[Close](#)

[Full Screen / Esc](#)

[Printer-friendly Version](#)

[Interactive Discussion](#)

and Koné et al. (2009) studied the dynamics of the surface bloom in the context of the bio-physical process in the IO using coupled bio-physical circulation model. In addition Resplandy et al. (2009) studied the seasonal and intraseasonal biogeochemical variability in the southern tropical IO using satellite observations and biophysical simulations.

More specifically in the EIO based on the silicate to carbonate ratio obtained from the sediment trap data Ramaswamy and Gaye (2006) showed that the foraminiferal carbonate is the major contributor to the biogenic flux and the reason for low productivity in the EIO was attributed to the dominance of carbonate producers. In fact, direct comparison of fluxes at southern Bay of Bengal trap (SBBT) and equatorial Indian Ocean trap (EIOT) revealed that carbonate fluxes were comparable at both sites, while opal fluxes as indicator for diatom production were much higher at SBBT (Unger and Jennerjahn, 2009). This is consistent with in situ measurements of Fernandes et al. (2008) who obtained low bacterial abundance as well as production in the EIO. Based on monthly mean climatology of chlorophyll pigment concentration Narvekar and Prasanna Kumar (2009) studied the seasonal cycle and showed that EIO had the least chlorophyll biomass compared to the Arabian Sea and the Bay of Bengal. More recently Sardesai et al. (2010) showed that the top 20 m of the water column close to Equator was devoid of nitrate irrespective of the season.

Though our understanding of the dynamics of the EIO has increased considerably over the years, information pertaining to the biogeochemistry of this region still remains very limited due to paucity of data. In the present study, using the biogenic flux data collected from the sediment trap mooring in the EIO, we explore (1) the role of physical and biological processes in mediating the observed variability and (2) coupling between the deep ocean biogenic flux and biological production at the upper ocean. Finally, we compare these with similar observations from the equatorial Pacific and the Atlantic oceans

2 Methodology and data sources

2.1 Study area

In the Indian Ocean, eight sediment trap moorings were deployed during the period 1986 to 1997 under Indo-German bilateral program to quantify the export of carbon from the ocean's surface into the ocean's interior (see Ittekkot, 1993; Rixen et al., 2009). For the present study we have selected sediment trap moorings that are located within the EIO. In order to define the latitudinal boundary of the EIO, we used monthly mean climatology of sea surface height anomaly (SSHA) (see Sect. 2.4 for details on SSHA) and subjected it to Fast Fourier Transformation (FFT) following Clark and Liu (1993). From the spatial distribution of the amplitude of the semi-annual signal (Fig. 1a) and the latitudinal distribution of zonal-averaged semi-annual amplitude (Fig. 1b) we define the region between 4.09° S and 5.57° N having the maximum amplitude as the EIO. See Clark and Liu (1993) for a similar argument to define the domain in the eastern equatorial region and Rao et al. (2009) for defining the equatorial wave guide.

Thus, we defined the region bounded by the broken line in Fig. 1b as the domain of EIO. Within this domain there are two moorings (Fig. 1a). The moorings located at 5° 24' N, 86° 46' E and at 3° 34' N, 77° 46' E are designated as southern Bay of Bengal trap (SBBT) and equatorial Indian Ocean trap (EIOT), respectively (see Rixen et al., 2009).

2.2 In situ data

2.2.1 Biogenic flux data

The biogenic flux data which contain organic carbon, calcium carbonate and biogenic silica were collected by using PARAFLEX Mark VI time-series sediment traps deployed at the SBBT (Unger et al., 2003) and EIO (Ramaswamy and Gaye, 2006). The SBBT data is for a period of ten years from November 1987 to December 1997, while the EIOT

BGD

10, 2889–2936, 2013

Seasonal cycle of biogenic flux in the equatorial Indian Ocean

P. J. Vidya et al.

Title Page

Abstract

Introduction

Conclusions

References

Tables

Figures

⏪

⏩

◀

▶

Back

Close

Full Screen / Esc

Printer-friendly Version

Interactive Discussion

Seasonal cycle of biogenic flux in the equatorial Indian Ocean

P. J. Vidya et al.

[Title Page](#)

[Abstract](#)

[Introduction](#)

[Conclusions](#)

[References](#)

[Tables](#)

[Figures](#)

[⏪](#)

[⏩](#)

[◀](#)

[▶](#)

[Back](#)

[Close](#)

[Full Screen / Esc](#)

[Printer-friendly Version](#)

[Interactive Discussion](#)



data is for one year period from January to December 1996. The sampling intervals at both the locations varied between 9 days to 42 days. Though two traps (shallow and deep) were deployed at each location, we used only shallow trap data for the present study as our aim is to understand the processes and coupling between the biological production in the euphotic zone and the mid-depth biogenic flux. The nominal depth of the shallow trap at SBBT was 1000 m while that at EIOT was 912 m. At first we converted this data in to respective calendar month for the entire period and from this the monthly mean climatology was generated to study the seasonal cycle at both the locations.

We are aware of the methodological shortcomings that are associated with flux measurements using sediment traps. Biases due to hydrodynamic flows over the trap mouth, particle transformation by bacteria and zooplankton as well as the influence of swimmers within the trap may lead to an under or overestimation of particle fluxes by a factor of up to 2. The calibration of particle fluxes with U-Th radionuclides has shown that fluxes at depths < 1000 m may be compromised because currents are stronger and zooplankton mainly migrates within this depth horizon (see Buesseler et al., 2007; Boyd and Trull, 2007). Depending on trap depth, sinking speed of particles and current speed, particles captured at one site may derive from a surface area as large as several hundreds of kilometers in diameter above the trap position. In addition to the large potential source area, the origin of particles might also vary in course of one year so that the obtained time series might represent export not from a defined but rather from a variable source region making it difficult to relate it to euphotic zone processes over the trap alone (Siegel and Deuser, 1997; Siegel et al., 1990, 2008; Waniek et al., 2005).

However, sediment traps are the only tool to monitor fluxes to a certain water depth continuously and over longer time spans and the usefulness of trap data have been proven by many studies showing that the observed fluxes actually relate to surface water processes. They are consistent with spatial variation of surface production and sediment properties (e.g. Jickells et al., 1996; Honjo et al., 1999; Waniek et al., 2005)

and reveal consistent seasonal as well as interannual variation driven by surface water processes (e.g. Waniek et al., 2005; Haake et al., 1996; Rixen et al., 2006; Holmes et al., 2002; Fischer et al., 1988; Wefer and Fischer, 1993; Voss et al., 1996).

For the SBBT site, consistent pattern of flux and composition prove that particle flux measured is suitable to characterize the relation between surface water processes and deep water particle fluxes both on seasonal as well as on interannual time scales (Unger et al., 2003, 2006). Limited data of ^{230}Th flux suggest that trap efficiency at SBBT is reasonably good (Sarin et al., 2000). In general, flux pattern persists throughout the water column, and for example the $\delta^{15}\text{N}$ signal hardly change with depth (Unger et al., 2006) indicating either that the particle sinking speed is sufficiently high to transport surface signals from a restricted region to depth, or that surface processes are not characterized by significant small scale variation. Less information is available for the EIOT site. Time coverage is much shorter. However, comparison with SBBT flux pattern reveals seasonal and episodic similarities between the two sites indicating that both sites are affected by the same surface ocean processes even though to a different extent (Unger and Jennerjahn, 2009).

2.2.2 Biological measurements

All the biological parameters used for the present study were measured during the cruise of ORV Sagar Kanya SK-227 during August 2006. Water samples from eight depths (0 m, 10 m, 20 m and thereafter every 20 m interval up to a depth of 120 m) were collected and analyzed for measurements of various biological parameters (see below). The data from stations 5°N and 83°E and 2.5°N and 77°E in the vicinity of

BGD

10, 2889–2936, 2013

Seasonal cycle of biogenic flux in the equatorial Indian Ocean

P. J. Vidya et al.

Title Page

Abstract

Introduction

Conclusions

References

Tables

Figures

⏪

⏩

◀

▶

Back

Close

Full Screen / Esc

Printer-friendly Version

Interactive Discussion

SBBT and EIOT, respectively were used for all the parameters except for the meso-zooplankton in the vicinity of SBBT which was from 2.5° N and 83° E.

Chlorophyll *a* (Fluorometric)

For estimation of total phytoplankton biomass (Chl *a*), 1L (litre) of water was filtered through the Whatman GF/F filter paper (47 mm diameter, 0.7 µm pore size) under low vacuum pressure. The pigments were extracted in 10 ml of 90% acetone in the dark for 24 h in the refrigerator. Fluorescence was measured before and after acidification with two drops of 1.2 N HCl following the JGOFS protocol (UNESCO, 1994).

Size fractionated chlorophyll *a*

Size fractionation of phytoplankton biomass was measured from selective depth (surface, chlorophyll maximum and 120 m depth) with the help of gravity filtration by serially passing water sample (5L) through 200, 60, 20 and 10 µm mesh. Finally filtrate was passed through 0.7 µm GF/F filters by applying very low vacuum. Particulate material retained on all of these filters was then analyzed following similar protocol as in TChl *a*. The percentage biomass was calculated for different fractions.

Primary productivity (PP)

Water samples from eight depths were transferred to four 300 mL capacity Nalgene Polycarbonate bottles (3 light and 1 dark). ¹⁴C was added (5 µCi; 185 kBq) to each bottle, and these bottles were incubated in situ at the respective depths from dawn to dusk (12 h). Incorporation of NaH¹⁴CO₃ by phytoplankton was determined following the

BGD

10, 2889–2936, 2013

Seasonal cycle of biogenic flux in the equatorial Indian Ocean

P. J. Vidya et al.

Title Page

Abstract

Introduction

Conclusions

References

Tables

Figures

⏪

⏩

◀

▶

Back

Close

Full Screen / Esc

Printer-friendly Version

Interactive Discussion

JGOFS Protocols (UNESCO, 1994). All samples were analyzed on a Packard 2500 TR (USA, Packard) scintillation counter.

Phytoplankton cell number

For qualitative and quantitative analysis of phytoplankton (size > 5 µm), 250 ml of water samples were collected from the euphotic zone (8 depths; 0–120 m) fixed in acid Lugol's iodine (1 % w/v) and preserved in 3 % formalin solution. The samples were stored in dark at low temperature until enumeration within a period of one month after collection. A settling and siphoning procedure was followed to obtain 50 ml concentrate. One ml in duplicates of this concentrate was then mounted on a Sedgwick Rafter counting chamber and examined through Olympus inverted microscope (magnification 100–200 ×). Generic and species identification was done according to various standard taxonomic keys (Subrahmanyam, 1946; Tomas, 1997; Lebour, 1978).

Meso-zooplankton

Samples were collected at mid-night using Multiple Plankton Closing Net (Hydro-Bios; mouth area 0.25 m²; mesh size 200 µm) equipped with a pre-calibrated flow meter. Five depths were sampled at each station: 1000–500 m, 500–300 m, 300-base of thermocline (BT), BT-top of thermocline (TT) and TT-surface (mixed layer). Samples are preserved in 5 % buffered formalin solution. Biomass was determined by displacement method. Depending on the size of the sample aliquots of 5–25 % were examined for microscopic identification and enumeration to the generic/species level using a stereo-zoom microscope.

Micro-zooplankton

For qualitative and quantitative analysis of microzooplankton, water samples were obtained from the same eight depths mentioned above for phytoplankton. Known volume (5 L) of water sample pre-filtered through 200 µm net was slowly passed through a wide

BGD

10, 2889–2936, 2013

Seasonal cycle of biogenic flux in the equatorial Indian Ocean

P. J. Vidya et al.

[Title Page](#)

[Abstract](#)

[Introduction](#)

[Conclusions](#)

[References](#)

[Tables](#)

[Figures](#)

[⏪](#)

[⏩](#)

[◀](#)

[▶](#)

[Back](#)

[Close](#)

[Full Screen / Esc](#)

[Printer-friendly Version](#)

[Interactive Discussion](#)



area of 20 μm net. The filtration was done carefully and slowly to avoid bursting of delicate forms due to pressure exerted while filtering. The filtered micro-zooplankton was then transferred to 100 mL GF/F filtered sea water and preserved with 1 % Acid Lugol's solution (with 2 mgL^{-1} of strontium sulphate) and 1 % EM Hexamine buffered formaldehyde. Samples were refrigerated in dark until analyzed later in the laboratory.

2.2.3 Hydrographic data

Monthly mean temperature and salinity data with resolution $1^\circ \times 1^\circ$ for the period 1987 January to 1997 December were obtained from the operational ocean reanalysis system (ORA – S3; Balmaseda et al., 2008) at European Centre for Medium-Range Weather Forecasts (ECMWF; http://apdrc.soest.hawaii.edu/datadoc/ecmwf_oras3.php) and computed MLD using 0.2 kgm^{-3} density criteria and also static stability of the water column was computed. The water column nitrate data for the month of August was taken from US National Oceanographic Data Centre (USNODC) for EIOT and from Indian Oceanographic Data Centre (IODC) for SBBT.

2.3 Reanalysis data

The monthly surface current data was taken from Ocean Surface Current Analysis – Real time (OSCAR) (<http://www.oscar.noaa.gov/>) during January 1993 to December 2010, which is real time reanalysis of currents averaged over the top 15 m with spatial resolution of $1^\circ \times 1^\circ$ (Bonjean et al., 2002). From these data the monthly mean climatology was computed. The zonal and meridional wind stress having a spatial resolution $1^\circ \times 1^\circ$, for the period January 1970 to December 2009 have been taken from the operational ocean reanalysis system (ORA – S3) (Balmaseda et al., 2008) at European Centre for Medium-Range Weather Forecasts (ECMWF; http://apdrc.soest.hawaii.edu/datadoc/ecmwf_oras3.php). Using this data zonal (u) and meridional wind (v) speeds, and Ekman pumping velocity (Gill, 1982) were computed.

BGD

10, 2889–2936, 2013

Seasonal cycle of biogenic flux in the equatorial Indian Ocean

P. J. Vidya et al.

Title Page

Abstract

Introduction

Conclusions

References

Tables

Figures

⏪

⏩

◀

▶

Back

Close

Full Screen / Esc

Printer-friendly Version

Interactive Discussion

2.4 Remote sensing data

In addition to the in situ data we also used remotely sensed satellite data. The monthly mean data on the chlorophyll *a* pigment concentrations and photosynthetically active radiation (PAR) were obtained from (oceansci.gsfc.nasa.gov/SeaWiFS/Mapped/Monthly/) Sea-viewing Wide Field-of-view Sensor (SeaWiFS) having a spatial resolution of 9 km for the period September 1997 to December 2010. Monthly mean sea surface height anomaly (SSHA) with spatial resolution $0.33^\circ \times 0.33^\circ$ for the period 1993 to 2010 was obtained from AVISO (www.aviso.oceanobs.com). Monthly mean sea surface temperature (SST) with resolution $1^\circ \times 1^\circ$ was taken from HadSST1.1 (www.metoffice.gov.uk/hadobs/hadisst/) period January 1970 to December 2009 (Rayner et al., 2003).

3 Results

The biogenic flux data used for the present study at SBBT is a monthly mean climatology that has been computed by taking the mean during the period 1987 to 1997. However, at EIOT we have only one year data from January to December of 1996. The obvious question is: will this be a representative flux data of EIOT? To explore whether 1996 is a normal year we compared the oceanic (SST), as well as the atmospheric (zonal and meridional components of the wind) parameters at EIOT with that of the climatology and presented it in Fig. 2 along with SD. The period from June to September is shaded in the figure as the focus is on the elevated biogenic flux at SBBT with that of EIOT during this period (see the following section). It is evident from the Fig. 2 that 1996 is well within 1SD of the climatology for all the three parameters considered. This gives us the confidence to consider the flux at EIOT during 1996 as representative.

BGD

10, 2889–2936, 2013

Seasonal cycle of biogenic flux in the equatorial Indian Ocean

P. J. Vidya et al.

Title Page

Abstract

Introduction

Conclusions

References

Tables

Figures

⏪

⏩

◀

▶

Back

Close

Full Screen / Esc

Printer-friendly Version

Interactive Discussion

3.1 Biogenic flux

The seasonal cycle of biogenic flux at SBBT showed strong seasonality in both climatology as well as atmospheric parameters for the year 1996 (Fig. 3). Since both followed similar pattern of seasonal variability, though with varying magnitudes, we limit our discussions to climatology. The average biogenic flux during January to May was $52.0 \text{ mg m}^{-2} \text{ d}^{-1}$, which showed an increasing trend from June to August and attained the maximum value of $160.9 \text{ mg m}^{-2} \text{ d}^{-1}$ in August. The lowest flux of $40.6 \text{ mg m}^{-2} \text{ d}^{-1}$ occurred in December. In contrast, no distinct seasonality could be deciphered at EIOT. In general, the biogenic flux at EIOT was lower than that at SBBT. During summer monsoon (June–September) the average biogenic flux at SBBT ($116.1 \pm 68.1 \text{ mg m}^{-2} \text{ d}^{-1}$) was about two-and-half times higher than that at EIOT ($42.9 \pm 18.2 \text{ mg m}^{-2} \text{ d}^{-1}$). The strong seasonality of biogenic flux at SBBT and lack of seasonality with very low flux at EIOT is intriguing considering the fact that both the traps were located within the equatorial region (see Fig. 1a) and hence expected to experience similar atmospheric forcing. Since it has been shown that the biogenic flux to the deeper ocean is to a large extent determined by the phytoplankton production in the euphotic zone (Honjo, 1982; Betzer et al., 1984; Waniek et al., 2005; Helmke et al., 2010; Lutz et al., 2010), as a first step we compared satellite derived chlorophyll concentrations to unravel the discrepancy between fluxes at both sites.

3.2 Satellite derived chlorophyll

In order to understand the relation between phytoplankton and biogenic flux at deeper ocean, we calculated the climatological monthly mean remotely sensed chlorophyll pigment concentration averaged within $1^\circ \times 1^\circ$ grid centered at SBBT and EIOT, respectively. It is pertinent to note that remotely sensed chlorophyll data reveals only the surface layer concentrations and will not be able to detect the presence of subsurface chlorophyll maxima (SCM). The chlorophyll pigment concentrations, though in general low, showed distinct seasonal cycle at both SBBT and EIOT (Fig. 4). Consistent

BGD

10, 2889–2936, 2013

Seasonal cycle of biogenic flux in the equatorial Indian Ocean

P. J. Vidya et al.

Title Page

Abstract

Introduction

Conclusions

References

Tables

Figures

⏪

⏩

◀

▶

Back

Close

Full Screen / Esc

Printer-friendly Version

Interactive Discussion

with the biogenic flux at SBBT the peak chlorophyll concentration occurred in August. The chlorophyll concentrations during January to April were low at both SBBT (0.13–0.18 mgm⁻³) and EIOT (0.13–0.19 mgm⁻³) and showed an increase from May attaining the maximum value of 0.34 and 0.27 mgm⁻³, respectively. Again, unlike the biogenic flux the chlorophyll during summer monsoon at SBBT (0.30 ± 0.08 mgm⁻³) and EIOT (0.25 ± 0.06 mgm⁻³) did not show large differences. From the close correspondence between the time variations of chlorophyll with that of biogenic flux at SBBT it would seem that they are closely coupled. However, at EIOT the seasonality of chlorophyll and lack of seasonality of biogenic flux would need an explanation. Before attempting to address this we explored the reason for (1) the observed seasonality in chlorophyll at both SBBT and EIOT and (2) lower chlorophyll at EIOT compared to SBBT during summer monsoon.

3.3 Photosynthetically active radiation (PAR)

Light, apart from nutrients, being one of the limiting factors for the growth of phytoplankton, we analyzed the PAR at both the locations. PAR showed a bimodal distribution at both SBBT (standard deviation 3.25 Em² d⁻¹) and EIOT (standard deviation 3.19 Em² d⁻¹) with a primary peak in March and a secondary peak in August (Fig. 5). Though PAR was high during summer at SBBT (45.7 Em² d⁻¹) compared to EIOT (43.8 Em² d⁻¹) the difference was less than the estimated bias (2.2 Em² d⁻¹, Frouin and Murakami, 2007). From the above it is evident that the marginal difference in PAR between SBBT and EIOT cannot account for the observed variability in the chlorophyll. The obvious reason for the variability in chlorophyll between SBBT and EIOT must be the difference in the availability of nutrients at these locations which in turn would depend upon the processes that make this nutrient available to the upper ocean.

The processes that could supply sub-surface nutrients to the upper ocean are the wind-mixing, Ekman-pumping, and advection which we examine in the following sections.

Seasonal cycle of biogenic flux in the equatorial Indian Ocean

P. J. Vidya et al.

Title Page

Abstract

Introduction

Conclusions

References

Tables

Figures

⏪

⏩

◀

▶

Back

Close

Full Screen / Esc

Printer-friendly Version

Interactive Discussion



3.4 Wind speed and static stability

The average wind speed during summer monsoon was higher in SBBT ($9 \pm 0.9 \text{ ms}^{-1}$) than in EIOT ($6 \pm 1.0 \text{ ms}^{-1}$) (Fig. 6). The higher winds would generally result in greater wind-mixing and the extent of this mixing depends on the stability of the water column. The static stability parameter [E] of the upper 200 m water column was calculated following Pond and Pickard (1978) and is given by

$$E \approx -\frac{1}{\rho} \frac{\partial \rho}{\partial z} \quad (1)$$

Where “ ρ ” is in situ density and z is the depth taken as negative. The static stability of the water column is analogous to potential energy, which is due to the virtue of its position. A positive value of “E” indicates that the water column is stable. If a parcel of water is displaced when the water column is stable, then the parcel will tend to return to its original position. On the other hand, if E is negative the water column is unstable and a displaced parcel of water will continue its displacement. When E is zero, the water column is neutrally stable. During August, static stability parameter at EIOT and SBBT showed similar positive values in the upper 40 m (Fig. 7) indicating a stable and stratified water column at both locations. Below this depth, “E” showed an increase up to 100 m followed by a decrease below it. Since the stability of water column in the upper 40 m was similar at EIOT and SBBT, an increase in the magnitude of the wind at SBBT during summer monsoon should lead to a greater mixing and make the mixed layer deeper compared to EIOT. An examination of mixed layer depth (MLD) showed that during August MLD was deepest at SBBT, which was 9m deeper than that at EIOT (Fig. 8). Thus, the stronger winds at SBBT during summer results in greater wind-mixing and this would presumably lead to an enhanced nutrient supply to the euphotic zone in SBBT compared to EIOT. To ascertain this we will examine the nitrate profiles in Sect. 3.7.

3.5 Ekman-pumping

To explore the role of Ekman-pumping in bringing about the observed changes in the chlorophyll the spatial distribution of monthly mean Ekman-pumping velocity, computed from the ECMWF reanalysis wind, were superimposed on to the chlorophyll a pigment concentrations for analysis for all the months from January to December (Fig. 9). The positive (negative) Ekman pumping velocity indicated the divergence (convergence) and upwelling (downwelling). During March-April the Ekman-pumping velocity in the vicinity of both SBBT and EIOT were zero with a chlorophyll value of 0.1 mg m^{-3} indicating oligotrophic regime. From June to September the Ekman-pumping velocity at SBBT and EIOT was negative indicating downwelling process. Hence, we infer that the observed enhanced chlorophyll in SBBT as well as EIOT during summer monsoon was not due to Ekman-pumping.

3.6 Horizontal advection

To understand the role of horizontal advection, we analyzed the spatial distribution of monthly mean climatology of chlorophyll pigment concentration overlaid with currents derived from OSCAR (Fig. 10). During summer monsoon (June–September) two strong currents were evident from the OSCAR data, the southward flowing West India coastal current (WICC) along the west coast of India (Shetye and Gouveia, 1998), and the eastward flowing southwest monsoon current (SMC) to the south. The strong WICC is capable of transporting chlorophyll from the phytoplankton bloom (Banse, 1987; Lierheimer and Banse, 2002) that occurs along the southern part of the west coast of India and Sri Lanka during summer monsoon. However, the spatial distribution of chlorophyll pigment concentration (Fig. 10) did not lend support to this as the location of both EIOT and SBBT was away from the region of high chlorophyll. Considering the large distances of both the trap locations from the coastal upwelling regions, we discount the role of advection in enhancing the chlorophyll.

BGD

10, 2889–2936, 2013

Seasonal cycle of biogenic flux in the equatorial Indian Ocean

P. J. Vidya et al.

Title Page

Abstract

Introduction

Conclusions

References

Tables

Figures

⏪

⏩

◀

▶

Back

Close

Full Screen / Esc

Printer-friendly Version

Interactive Discussion

3.7 Nitrate profiles

The vertical distribution of nitrate in the upper 120 m of the water column at SBBT and EIOT during August showed that surface water at SBBT had nitrate in excess of $0.3 \mu\text{M}$ (Fig. 11a). In contrast, at EIOT the nitrate value near surface (3 m) was $0.1 \mu\text{M}$. At 40 m SBBT had a nitrate concentration of $1.95 \mu\text{M}$ as against $0.88 \mu\text{M}$ in EIOT. Recall that MLD at SBBT and EIOT was 50 m and 41 m, respectively. Since MLD was deeper than the top-of-nitracline at SBBT, a strong wind-mixing would support a higher chlorophyll biomass through entrainment compared to EIOT where nitracline was deeper than MLD and winds were comparatively weaker.

Thus, from the above it is clear that the physical process that led to the enhancement of chlorophyll at both SBBT and EIOT was the wind-mixing and subsequent nutrient entrainment into the upper ocean. To understand the processes that led to the observed lower biogenic flux in the EIOT compared to SBBT we examined the biological parameters.

3.8 In situ chlorophyll *a*

The vertical profile of in situ chlorophyll *a* (Chl *a*) in August 2006 showed the presence of a characteristic subsurface chlorophyll maximum (SCM) at both the regions (Fig. 11b). At SBBT, the SCM was seated at 20 m and had a chlorophyll concentration (0.61 mg m^{-3}) almost twice that of surface (0.36 mg m^{-3}). The SCM contributed 29 % of the total chlorophyll in the upper 120 m water column whereas the surface biomass contributed only to 14 % of the total. At EIOT the SCM was located at 60 m depth and had a chlorophyll biomass (0.36 mg m^{-3}) which was six times higher than that of surface concentration (0.06 mg m^{-3}). The SCM contributed 34 % of the total chlorophyll in the upper 120 m water column at EIOT whereas surface chlorophyll contributed to 6 %.

The Overall, the integrated chlorophyll *a* concentration in the upper 120 m at SBBT was much higher (29.6 mg m^{-2}) than that at EIOT (18.7 mg m^{-2}). The major difference in biomass was in the upper 60 m of the water column.

3.9 Primary production

The vertical profiles of primary production (PP) showed much higher PP at SBBT compared to EIOT (Fig. 11c). Surface PP at SBBT ($1.59 \text{ mg C m}^{-3} \text{ d}^{-1}$) was four times higher than that of EIOT ($0.38 \text{ mg C m}^{-3} \text{ d}^{-1}$). The subsurface PP-maximum was seen at 10 m at SBBT ($8.4 \text{ mg C m}^{-3} \text{ d}^{-1}$). The EIOT showed two maxima – the first one at 10 m ($2.56 \text{ mg C m}^{-3} \text{ d}^{-1}$) and the second one at 60 m – which were comparable. The column integrated (120 m) PP values at SBBT ($353.6 \text{ mg C m}^{-2} \text{ d}^{-1}$) were more than three times higher than those at EIOT ($108.4 \text{ mg C m}^{-2} \text{ d}^{-1}$).

3.10 Phytoplankton abundance and assemblage

The phytoplankton abundance (Fig. 12a) and composition at SBBT and EIOT was analyzed to understand community structure and its spatial variation (Table 1). Numerical abundance showed a subsurface maximum at SBBT which was located at 40 m with a value of $2576 \text{ cells L}^{-1}$. This was 8 times higher than the maxima at EIOT located at 10 m and 60 m with a value of 330 cells L^{-1} (Fig. 12a). Further, the phytoplankton community was largely dominated by diatoms which was 8-times higher compared to EIOT (Table 1).

The phytoplankton community (diatom and dinoflagellates) was also found to be more diverse at SBBT (20 genera) as compared to EIOT (9 genera). The dominant forms at SBBT were *Rhizosolenia styliformis* (16.9%), *Pseudonitzschia turgidula* (9.2%), *Chaetoceros didymus* (6%), *Nitzschia delicatissima* (5%) whereas *Leptocylindrus danicus* (28%), *Synedra* spp. (7.8%), *Nitzschia* spp. (5.4%), *Thalassiothrix longissima* (4.7%) dominated EIOT stations. Among dinoflagellates that contributed less than 10% includes *Gymnodinium* spp. (3%) and *Prorocentrum micans* (1.9%) at SBBT while *Ceratium trichoceros* (2.7%) and *Phalacroma circumsutum* (1.9%) dominated EIOT.

BGD

10, 2889–2936, 2013

Seasonal cycle of biogenic flux in the equatorial Indian Ocean

P. J. Vidya et al.

Title Page

Abstract

Introduction

Conclusions

References

Tables

Figures

⏪

⏩

◀

▶

Back

Close

Full Screen / Esc

Printer-friendly Version

Interactive Discussion

3.11 Mesozooplankton biomass

The mesozooplankton biomass in upper 1000 m was largely dominated by copepods which are 2-fold higher at SBBT (24.47 mLm^{-3}) than at EIOT (14.7 mLm^{-3}). Vertically, the highest biomass was concentrated in the MLD (0–60 m Fig. 12b). In the upper 300 m also the mesozooplankton biomass at EIOT was lower than that at SBBT.

3.12 Microzooplankton

The microzooplankton was largely comprised of Protozoans, particularly ciliates and flagellates. We considered microzooplankton abundance along with mesozooplankton biomass as an added parameter, to have a basic understanding about the system and about the kind of food web that might be functional in SBBT and EIOT. Spatial variation in microzooplankton abundance along 77° E (EIOT) and 83° E (SBBT) showed high microzooplankton abundance at EIOT ($1000 \text{ organisms L}^{-1}$) compared to SBBT ($500\text{--}600 \text{ organisms L}^{-1}$) (Fig. 12c).

3.13 Size fractionated chlorophyll *a*

Size fractionated chlorophyll *a* along 77° E (5° N and at Equator) as shown in Fig. 13, which indicate that the pico-phytoplanktons ($< 10 \mu\text{m}$ but $> 0.7 \mu\text{m}$) dominated the phytoplankton biomass at all the depths (Fig. 13). At selected depths (surface, SCM, and 120 m) picophytoplankton accounted for 79 %, 94 %, 66 % at 5° N and 93 %, 94 %, and 70 % at Equator, respectively.

4 Discussion

The characteristic feature of the mid-depth biogenic flux at SBBT was strong seasonality with peak flux during summer monsoon (June–September), which was observed regularly over the period 1988–1997 (Unger et al., 2006). In contrast, EIOT showed

BGD

10, 2889–2936, 2013

Seasonal cycle of biogenic flux in the equatorial Indian Ocean

P. J. Vidya et al.

Title Page

Abstract

Introduction

Conclusions

References

Tables

Figures

⏪

⏩

◀

▶

Back

Close

Full Screen / Esc

Printer-friendly Version

Interactive Discussion



Seasonal cycle of biogenic flux in the equatorial Indian Ocean

P. J. Vidya et al.

[Title Page](#)

[Abstract](#)

[Introduction](#)

[Conclusions](#)

[References](#)

[Tables](#)

[Figures](#)

[⏪](#)

[⏩](#)

[◀](#)

[▶](#)

[Back](#)

[Close](#)

[Full Screen / Esc](#)

[Printer-friendly Version](#)

[Interactive Discussion](#)



a consistently low flux without any seasonality, the flux being two-and-half times less than that of SBBT. This large difference appears to be an anomaly as both EIOT and SBBT traps were located within the equatorial region which experiences similar atmospheric forcing. The observed differential biogenic flux at SBBT and EIOT could be understood in the context of prevailing physical as well as biological processes at these locations, both of which influence the chlorophyll biomass. At any given location chlorophyll biomass depends on the availability of sunlight and nutrients (bottom-up control) and grazing (top-down control). The bottom-up control in turn is controlled by physical processes. We first examined the physical process to understand the observed variability in the chlorophyll biomass and then the processes that control the biogenic flux to the deeper ocean.

The time evolution of satellite derived chlorophyll, unlike the biogenic flux, showed distinct seasonality at both SBBT and EIOT. Though the peak chlorophyll occurred during summer monsoon, the magnitude at SBBT was marginally higher than that at EIOT. The in situ measurements of chlorophyll *a* in August 2006 also showed a similar result. The column integrated chlorophyll *a* as well as PP was also higher near SBBT compared to EIOT, the former was one-and-half times higher. An examination of PAR showed only a marginal difference between the two locations. The time evolution of wind speed showed good correspondence with chlorophyll. Higher winds at SBBT than at EIOT during summer monsoon indicated the role of wind-mixing in supplying the nutrients to the upper ocean. However, the amount of nutrient supply will depend upon the stability of the upper water column and the vertical gradient. Since the static stability of water column in the upper 40 m at SBBT and EIOT during August was comparable, a stronger wind at SBBT should lead to a greater mixing. An examination of the mixed layer as well as the nitrate profile during August showed that (1) MLD at SBBT was deeper than that at EIOT, (2) top-of-nitracline was within the MLD at SBBT, while it was deeper than MLD at EIOT and (3) at 40 m the nitrate concentrations at SBBT was twice higher than that at EIOT. Hence, though the wind-mixing during summer monsoon supplied nutrients to the upper ocean at both locations, the stronger winds at SBBT

Seasonal cycle of biogenic flux in the equatorial Indian Ocean

P. J. Vidya et al.

[Title Page](#)

[Abstract](#)

[Introduction](#)

[Conclusions](#)

[References](#)

[Tables](#)

[Figures](#)

[⏪](#)

[⏩](#)

[◀](#)

[▶](#)

[Back](#)

[Close](#)

[Full Screen / Esc](#)

[Printer-friendly Version](#)

[Interactive Discussion](#)

compared to EIOT resulted in greater entrainment of nutrients to the euphotic zone in SBBT. Thus, the observed enhancement of chlorophyll during summer monsoon at both SBBT and EIOT resulted from wind-driven entrainment bloom. The magnitude of the chlorophyll enhancement was controlled by the vertical distribution of nitrate and strength of the wind. However, this does not explain the mismatch between the biogenic flux and chlorophyll at EIOT.

In the light of the inadequacy of the bottom-up control to explain the mismatch between the chlorophyll biomass and biogenic flux during summer monsoon, we examined the longitudinal differences in the prevailing plankton community and the associated biological processes that operate at these locations. Buesseler (1998) reported a decoupling between primary production and export of organic carbon to the deep and found that high export rates were mostly related to diatom based food webs. Against this background we used available in situ data of nitrate, chlorophyll *a*, primary productivity (PP), phytoplankton cell number, meso-zooplankton biomass and micro-zooplankton that were collected near SBBT and EIOT during August 2006 as a part of the equatorial Indian Ocean Process Study (EIOPS) programme (Prasanna Kumar et al., 2010) to evaluate food web structure at the respective sites. Glover et al. (1985) showed that when the productivity maximum occurs at depth shallower than SCM, there will be a dominance of larger phytoplankton cells. Hasle and Syvertsen (1997) noticed that whenever high chlorophyll as well as larger phytoplankton cells ($> 5 \mu\text{m}$) were supported by the new nitrogen, diatom would dominate over the other phytoplankton. We encountered a similar situation at SBBT where productivity maximum was at much shallower depth than SCM. Further, our results based on microscopic as well as size fractionated chlorophyll *a* studies showed that the cell count of larger ($> 5 \mu\text{m}$) phytoplankton was dominated by diatoms at SBBT and was several times higher than that compared to EIOT. We presume that the higher cell count of larger phytoplankton at SBBT was supported by the higher concentration of new nitrogen made available by strong wind-mixing. The meso-zooplankton biomass at SBBT in the upper 300 m was more than twice that at EIOT, while the micro-zooplankton at SBBT was one-and-half

times less than that at EIOT. Thus, the dominance of diatom and meso-zooplankton over micro-zooplankton at SBBT suggested the prevalence of classical food web. The resulting export could be both via aggregation following a diatom bloom and through fecal pellets due to meso-zooplankton grazing.

5 In contrast, at EIOT, the peaks of both primary productivity and chlorophyll *a* at EIOT were at 60m located in the low light region, which indicated the prevalence of picophytoplankton (see Glover et al., 1985; Platt et al., 1983). Our size fractionated chlorophyll *a* also showed that the enhanced phytoplankton biomass at EIO was dominated by pico-phytoplankton. The high micro zooplankton abundance and lesser
10 meso-zooplankton biomass at EIOT indicated the importance of the microbial loop in the microbial component. This food web is believed to be more efficient at re-cycling (Beatriz et al., 2001) and is generally associated with low export.

Having explored the physical and biological processes that control the biogenic fluxes in the SBBT and EIOT, it is important to quantitatively compare the export of organic carbon at these locations with that of the equatorial Pacific and Atlantic. At SBBT, the biogenic flux accounts for 45.5% of the primary production (Table 2). A comparison of similar values in the equatorial Atlantic showed that 43.2% of the primary production during August/September ($500 \text{ mg C m}^{-2} \text{ d}^{-1}$) (Voituriez and Herbrand, 1981) accounted for the biogenic flux of $216.1 \text{ mg m}^{-2} \text{ d}^{-1}$ (Fischer and Wefer, 1991). However, the organic carbon export in the SBBT was 3.4% while that in the equatorial Atlantic was 6% (Table 2). This is understandable, as strong upwelling in the equatorial Atlantic (Monger et al., 1997) supplies enough new nutrients to the euphotic zone to support greater diatom growth compared to SBBT where the new nitrogen is supplied by wind-driven entrainment. This faster sinking diatom (Bradtmiller et al., 2007) contributes to the high flux in the equatorial Atlantic. Hence, the processes at SBBT could be similar to that operating in the equatorial Atlantic. In contrast, biogenic flux at EIOT was $37.5 \text{ mg m}^{-2} \text{ d}^{-1}$ (Table 2), which accounted for only 13% of the primary production ($288.2 \text{ mg C m}^{-2} \text{ d}^{-1}$) and the calculated organic carbon export was also found to be low (2%). This could best be explained through the “microbial loop” in the microbial food

Seasonal cycle of biogenic flux in the equatorial Indian Ocean

P. J. Vidya et al.

[Title Page](#)[Abstract](#)[Introduction](#)[Conclusions](#)[References](#)[Tables](#)[Figures](#)[⏪](#)[⏩](#)[◀](#)[▶](#)[Back](#)[Close](#)[Full Screen / Esc](#)[Printer-friendly Version](#)[Interactive Discussion](#)

Seasonal cycle of biogenic flux in the equatorial Indian Ocean

P. J. Vidya et al.

[Title Page](#)

[Abstract](#)

[Introduction](#)

[Conclusions](#)

[References](#)

[Tables](#)

[Figures](#)

[⏪](#)

[⏩](#)

[◀](#)

[▶](#)

[Back](#)

[Close](#)

[Full Screen / Esc](#)

[Printer-friendly Version](#)

[Interactive Discussion](#)



web (Madhupratap et al., 1996; Gauns et al., 2000). This is comparable to the situation in the equatorial Pacific where the total biogenic flux during August/September showed a maximum value of $88.6 \text{ mg m}^{-2} \text{ d}^{-1}$ and the primary production was $500 \text{ mg C m}^{-2} \text{ d}^{-1}$ (Honjo et al., 1995), indicating that only 17.2% of the primary productivity is transferred to the ocean interior in the form of biogenic flux (Table 2); the organic carbon export was 0.9%. From the above we surmise that the process operating in the EIOT may be similar to that of the equatorial Pacific. The difference being lack of upwelling at EIOT that leads to much less primary production compared to the equatorial Pacific.

Thus, the high biogenic flux at SBBT was supported by the faster sinking of diatoms as well as through fecal pellets of mesozooplankton (classical food web), a process similar to that of equatorial Atlantic. This is also evident in the direct comparison of opal and carbonate fluxes at SBBT and EIOT, which showed comparable carbonate fluxes, while opal fluxes were significantly higher at SBBT (Unger and Jennerjahn, 2009). This difference in fluxes is also mirrored in the phytoplankton community, which was more diverse near SBBT (20 genera) as compared to that near EIOT (9 genera) wherein, large standing stock of picoautotrophs expectedly consumed by protozoa (ciliates, flagellates), dominant forms of microzooplankton (Madhupratap et al., 1996; Gauns et al., 2000). This is also reflected in the comparatively higher foraminifera fluxes at the EIOT site (Ramaswamy and Gaye, 2006). Further, foraminifera are part of the microplankton taxa, suggesting their importance (possibly through grazing) in the microbial components of the region. Thus, at EIOT most of the photosynthetically produced organic matter is remineralized within the upper ocean leaving very little carbon to sink (Williams, 1998), a situation similar to that of the equatorial Pacific. Finally, we present a schematic picture (Fig. 14) that depicts the above discussed processes starting from production of organic carbon in the upper ocean to its export into the deep ocean as captured by the sediment trap at SBBT and EIOT and its comparison with equatorial Atlantic and Pacific oceans.

5 Concluding remarks

Sediment trap data from the equatorial Indian Ocean region provided an insight into the processes that link the primary production to the sinking organic carbon in which physical and biological processes are intimately coupled. Our study demonstrates that, though SBBT and EIOT are within the same geographical entity, the processes that control the primary production in the euphotic zone and the biogenic flux to the deep ocean are very different. We see a striking similarity between the biological process operating at EIOT with that of equatorial Pacific, and SBBT with that of the equatorial Atlantic, though the physical forcing in these three regions are very different. There are some uncertainties in our study, especially the role of meso-zooplankton grazing, which needs to be quantified. We also would need data on dissolved organic carbon to have a better handle on the microbial food web.

Acknowledgements. The authors thank Director National Institute of Oceanography (NIO) Goa and Council of Scientific and Industrial Research (CSIR), New Delhi for all support and encouragement. They express their gratitude to R. Antao (retired), Department of English, Dhempe College of Arts and Science, Panaji, Goa for meticulously going through the manuscript and suggesting language corrections. All the participants of ORV Sagar Kanya cruise 227 are acknowledged for their help in data collection and analysis. Ms. Vidya acknowledges CSIR for Senior Research Fellowship. This is NIO contribution number xxxx.

References

- Anderson, D. L. T. and Carrington, D. J.: Modeling interannual variability in the Indian Ocean using momentum fluxes from the operational weather analysis of the UK Meteorological Office and European Centre for Medium Range Weather Forecasts, *J. Geophys. Res.*, 98, 12483–12499, 1993.
- Asper, V. L., Deuser, W. G., Knauer, G. A., and Lohrenz, S. E.: Rapid coupling of sinking particle fluxes between surface and deep ocean waters, *Nature*, 357, 670–672, 1992.

BGD

10, 2889–2936, 2013

Seasonal cycle of biogenic flux in the equatorial Indian Ocean

P. J. Vidya et al.

Title Page

Abstract

Introduction

Conclusions

References

Tables

Figures



Back

Close

Full Screen / Esc

Printer-friendly Version

Interactive Discussion

Seasonal cycle of biogenic flux in the equatorial Indian Ocean

P. J. Vidya et al.

[Title Page](#)

[Abstract](#)

[Introduction](#)

[Conclusions](#)

[References](#)

[Tables](#)

[Figures](#)

[⏪](#)

[⏩](#)

[◀](#)

[▶](#)

[Back](#)

[Close](#)

[Full Screen / Esc](#)

[Printer-friendly Version](#)

[Interactive Discussion](#)



- Balmaseda, M. A., Vidard, A., and Anderson, D. L. T.: The ECMWF Ocean Analysis System: ORA-S3, *Mon. Weather Rev.*, 136, 3018–3034, 2008.
- Banse, K.: Seasonality of phytoplankton chlorophyll in the central and northern Arabian Sea, *Deep-Sea Res.*, 34 713–723, 1987.
- 5 Beatriz, M. B., Fasham, M. J. R., and Bowles, M. C.: Ocean Biogeochemistry and Global Change: JGOFS Research Highlights 1988–2000, IGBP Science Series 2, SCOR, IGBP, National Science Foundation, Research Council of Norway, University of Bergen, 36 pp., 2001.
- Betzer, P. R., Showers, W. J., Laws, E. A., Winn, C. D., DiTullio, G. R., and Kroopnick, P. M.:
 10 Primary productivity and particle fluxes on a transect of the Equator at 153° W in the Pacific Ocean, *Deep-Sea Res.*, 31, 1–11, 1984.
- Bishop, J. K. B.: Regional extremes in particulate matter composition and flux: effects on the chemistry of the ocean interior, in: *Productivity of the Ocean: Present and Past*, edited by: Berger, W. H., Smetacek, V. S. and Wefer, G., J. Wiley and Sons, Chichester, UK, 117–137,
 15 1989.
- Bonjean, F. and Lagerloef, G. S. E.: Diagnostic model and analysis of the surface currents in the tropical Pacific Ocean, *J. Phys. Oceanogr.*, 32, 2938–2954, 2002.
- Boyd, P. W. and Trull, T. W.: Understanding the export of biogenic particles in oceanic waters: is there consensus?, *Prog. Oceanogr.*, 72, 276–312, doi:10.1016/j.pocean.2006.10.007, 2007.
- 20 Bradtmiller, L. I., Anderson, R. F., Fleisher, M. Q., and Burckle, L. H.: Opal burial in the equatorial Atlantic Ocean over the last 30 ka: implications for glacial–interglacial changes in the ocean silicon cycle, *Paleoceanography*, 22, PA4216, doi:10.1029/2007PA001443, 2007.
- Bubnov, V. A.: Climatic zonal pressure gradient in the equatorial zone of the Indian Ocean, *Oceanology*, 33, 414–420, 1994.
- 25 Buesseler, K. O.: The decoupling of production and particulate export in the surface ocean, *Global Biogeochem. Cy.*, 12 297–310, 1998.
- Buesseler, K. O., Antia, A. N., Chen, M., Fowler, S. W., Gardner, W. D., Gustafsson, O., Harada, K., Michaels, A. F., Rutgers van der Loeff, M., Sarin, M., Steinberg, D. K., and Trull, T.: An assessment of the use of sediment traps for estimating upper ocean particle
 30 fluxes, *J. Mar. Res.*, 65, 345–416, 2007.
- Carr, M.-E., Friedrichs, M. A. M., Schmeltz, M., Aita, M. N., Antoine, D., Arrigo, K. R., Asanuma, I., Aumont, O., Barber, R., Behrenfeld, M., Bidigare, R., Buitenhuis, E. T., Cambell, J., Ciotti, A., Dierssen, H., Dowell, M., Dunne, J., Esaias, W., Gentili, B.,

Seasonal cycle of biogenic flux in the equatorial Indian Ocean

P. J. Vidya et al.

[Title Page](#)

[Abstract](#)

[Introduction](#)

[Conclusions](#)

[References](#)

[Tables](#)

[Figures](#)

[⏪](#)

[⏩](#)

[◀](#)

[▶](#)

[Back](#)

[Close](#)

[Full Screen / Esc](#)

[Printer-friendly Version](#)

[Interactive Discussion](#)

Gregg, W., Groom, S., Hoepffner, N., Ishizaka, J., Kameda, T., LeQuéré, C., Lohrenz, S., Marra, J., Mélin, F., Moore, K., Morel, A., Reddy, T. E., Ryan, J., Scardi, M., Smyth, T., Turpie, K., Tilstone, G., Waters, K., and Yamanaka, Y.: A comparison of global estimates of marine primary production from ocean color, *Deep-Sea Res. Pt. II*, 533, 741770, doi:10.1016/j.dsr2.2006.01.028, 2006.

Clarke, A. J. and Liu, X.: Observations and dynamics of semiannual and annual sea levels, *J. Phys. Oceanogr.*, 23, 386–399, 1993.

Fernandes, V., Rodrigues, V., Ramaiah, N., and Paul, J. T.: Relevance of bacterioplankton abundance and production in the oligotrophic equatorial Indian Ocean, *Aquat. Ecol.*, 42, 511–519, 2008.

Fischer, G. and Wefer, G.: Sampling, preparation and analysis of marine particulate matter, in: *Marine Particles: Analysis and Characterization*, edited by: Hurd, D. C. and Spencer, D. W., *Geophysical Monographs*, 391–397 pp., 1991.

Fischer, G., Fütterer, D., Gersonde, R., Honjo, S., Ostermann, D., and Wefer, G.: Seasonal variability of particle flux in the Weddell Sea and its relation to ice cover, *Nature*, 335, 426–428, 1988.

Frouin, R. and Murakami, H.: Estimating photosynthetically available radiation at the ocean surface from ADEOS-II Global Imager data, *J. Oceanogr.*, 63, 493–503, 2007.

Gauns, M.: Role of microzooplankton in the food chain dynamics of some tropical marine environments, Ph.D. thesis, Goa University, India, 2007.

Gent, P. R., O'Neill, K., and Cane, M. A.: A model of the semiannual oscillation in the equatorial Indian Ocean, *J. Phys. Oceanogr.*, 13, 2148–2160, 1983.

Gonella, J., Reverdin, G., and Fioux, M.: Dynamical oceanography-hypothesis in favour of the genesis of the equatorial oceanic jet of the Indian Ocean by attenuation of the Somalian eddy after the end of the south-west monsoon, *C. R. Acad. Sci. Paris*, 29, 899–902, 1983.

Gill, A. E.: *Atmosphere Ocean Dynamics*, Academic Press, London, UK, 662 pp., 1982.

Glover, H. E., Phinney, D. A., and Yentsch, C. S.: Photosynthetic characteristics of picoplankton compared with those of larger phytoplankton populations, in various water masses in the Gulf of Maine, *Biol. Oceanogr.*, 3, 223–248, 1985.

Hakke, B., Rixen, T., Reemtsma, T., Ramaswamy, V., and Ittillot, V.: Processes determining seasonality and interannual variability of settling particle fluxes to the deep Arabian Sea, in: *Particle Flux in the Ocean*, edited by: Ittekkot, V., Schafer, P., Honjo, S., and Depetris, John Wiley, Chichester, UK, 251–270, 1996.

Seasonal cycle of biogenic flux in the equatorial Indian Ocean

P. J. Vidya et al.

[Title Page](#)

[Abstract](#)

[Introduction](#)

[Conclusions](#)

[References](#)

[Tables](#)

[Figures](#)

[⏪](#)

[⏩](#)

[◀](#)

[▶](#)

[Back](#)

[Close](#)

[Full Screen / Esc](#)

[Printer-friendly Version](#)

[Interactive Discussion](#)

- Han, W., McCreary, J. P., Anderson, J. D. L. T., and Mariano, A. J.: On the dynamics of the eastward surface jets in the equatorial Indian Ocean, *J. Phys. Oceanogr.*, 29, 2191–2209, 1999.
- Harris, G. P.: *Phytoplankton Ecology: Structure, Function and Fluctuation*, 1st edn., Chapman & Hall, London, 1986.
- Hastenrath, S. and Greischar, L.: The monsoonal heat budget of the hydrosphere-atmosphere system in the Indian Ocean sector, *J. Geophys. Res.*, 98, 6869–6881, 1989.
- Hasle, G. R. and Syvertsen, E. E.: Marine diatoms, in: *Identifying Marine Diatoms and Dinoflagellates*, edited by: Tomas, C. R., Academic Press, San Diego, 3–385, 1997.
- Helmke, P., Neuer S., Lomas M. W., Conte, M., and Freudenthal, T.: Cross-basin differences in particulate organic carbon export and flux attenuation in the subtropical north Atlantic gyre, *Deep-Sea Res. Pt. I*, 57, 213–227, 2010.
- Holmes, R. M., McClelland, J. W., Peterson, B. J., Shiklomanov, I. A., Shiklomanov, A. I., Zhulidov, A. V., Gordeev, V. V., and Bobrovitskaya, N. N.: A circumpolar perspective on fluvial sediment flux to the Arctic Ocean, *Global Biogeochem. Cy.*, 16, 1–14, doi:10.1029/2001GB001849, 2002.
- Honjo, S.: Seasonality and interaction of biogenic and lithogenic particulate flux at the Panama Basin, *Science*, 218, 883–884, 1982.
- Honjo, S., Dymond, J., Collier, R., and Manganini, S. J.: Export production of particles to the interior of the equatorial Pacific Ocean during the 1992 EqPac experiment, *Deep-Sea Res. Pt. II*, 42, 831–870, 1995.
- Honjo, S., Dymond, J., Prell, W., and Ittekkot, V.: Monsoon-controlled export fluxes to the interior of the Arabian Sea, *Deep-Sea Res. Pt. II*, 46, 1859–1902, 1999.
- Ittekkot, V.: The abiotically driven biological pump in the ocean and short-term fluctuations in atmospheric CO₂ contents, *Global Planet. Change*, 8, 17–25, 1993.
- Jickells T. D, Newton P. P., King P., Lampitt, R. S., and Boutle, C.: A comparison of sediment trap records of particle fluxes from 19 to 48° N in the northeast Atlantic and their relation to surface water productivity, *Deep-Sea Res. Pt. I*, 43, 971–986, 1996.
- Knauss, J. A.: Measurements of the Cromwell Current, *Deep-Sea Res.*, 6, 265–286, 1960.
- Koné, V., Aumont, A., Lévy, M., and Resplandy, L.: Physical and biogeochemical controls of the phytoplankton seasonal cycle in the Indian Ocean: a modeling study, *Geoph. Monog. Series*, 185, 147–166, doi:10.1029/2008GM000700, 2009.

Seasonal cycle of biogenic flux in the equatorial Indian Ocean

P. J. Vidya et al.

[Title Page](#)

[Abstract](#)

[Introduction](#)

[Conclusions](#)

[References](#)

[Tables](#)

[Figures](#)

[⏪](#)

[⏩](#)

[◀](#)

[▶](#)

[Back](#)

[Close](#)

[Full Screen / Esc](#)

[Printer-friendly Version](#)

[Interactive Discussion](#)



- Knox, R. A.: On a long series of the Indian Ocean equatorial currents near Addu Atoll, *Deep-Sea Res.*, 23, 211–221, 1976.
- le B. Williams, P. J.: The balance of plankton respiration and photosynthesis in the open ocean, *Nature*, 394, 55–57, 1998.
- 5 Lebour, M.: *The Planktonic Diatom of Northern Seas*, Otto Koeltz Science Publishers, Koenigstein/Germany, 25–215, 1978.
- Leetma, A. and Stommel, H.: Equatorial current observations in the western Indian Ocean in 1975 and 1976, *J. Phys. Oceanogr.*, 10, 258–269, 1980.
- Lévy, M., D. Shankar, D., André, J. M., Shenoi, S. S. C., Durand, F., and de Boyer Montégut, C.: Basin-wide seasonal evolution of the Indian Ocean's phytoplankton blooms, *J. Geophys. Res.*, 112, C12014, doi:10.1029/2007JC004090, 2007.
- 10 Lierheimer, L. J. and Banse, K.: Seasonal and interannual variability of phytoplankton pigment in the Laccadive (Lakshadweep) Sea as observed by the Coastal Zone Color Scanner, *P. Indian A. S.-Earth*, 111, 163–185, 2002.
- 15 Longhurst, A.: Seasonal cycles of pelagic production and consumption, *Prog. Oceanogr.*, 36, 77–167, 1995.
- Lutz, M., Dunbar, R., and Caldiera, K.: Regional variability in the vertical flux of articulate organic carbon in the ocean interior, *Global Biogeochem. Cy.*, 16, 1037, doi:10.1029/2000GB001383, 2002.
- 20 Lutz V. A., Segura, V., Dogliotti, A. I., Gagliardini, D. A., Bianchi, A. A., and Balestrini, C. E.: Primary production in the Argentine Sea during spring estimated by field and satellite models, *J. Plankton Res.*, 32, 181–195, 2010.
- Luyten, J. R. and Roemmich, D. H.: Equatorial currents at semiannual period in the Indian Ocean, *J. Phys. Oceanogr.*, 12, 406–413, 1982.
- 25 Madhupratap, M., Prasanna Kumar, S., Bhattathiri, P. M. A., Dileep Kumar, M., Raghukumar, S., Nair, K. K. C., and Ramaiah, N.: Mechanism of the biological response to winter cooling in the northeastern Arabian Sea, *Nature*, 384, 549–552, 1996.
- Masumoto, Y., Hase, H., Kuroda, Y., Matsuura, H., and Takeuchi, K.: Intraseasonal variability in the upper layer currents observed in the eastern equatorial Indian Ocean, *Geophys. Res. Lett.*, 32, L02607, doi:10.1029/2004GL021896, 2005.
- 30 McCreary, J. P., Kundu, P. K., and Molinari, R. L.: A numerical investigation of dynamics, thermodynamics, and mixed-layer processes in the Indian Ocean, *Prog. Oceanogr.*, 31, 181–224, 1993.

Seasonal cycle of biogenic flux in the equatorial Indian Ocean

P. J. Vidya et al.

[Title Page](#)

[Abstract](#)

[Introduction](#)

[Conclusions](#)

[References](#)

[Tables](#)

[Figures](#)

[⏪](#)

[⏩](#)

[◀](#)

[▶](#)

[Back](#)

[Close](#)

[Full Screen / Esc](#)

[Printer-friendly Version](#)

[Interactive Discussion](#)

- McCreary, J. P., Murtugudde, R., Vialard, J., Vinayachandran, P. N., Wiggert, J. D., Hood, R. R., Shankar, D., and Shetye, S. R.: Biophysical processes in the Indian Ocean, edited by: Wiggert, J. D., Hood, R. R., Naqvi, S. W. A., Brink, K. H., and Smith, S. L., Geoph. Monog. Series, American Geophysical Union, Washington, DC, 9–32, doi:10.1029/2008GM000768, 2009.
- 5 Monger, B., McClain, C. R., and Murtugudde, R. G.: Seasonal phytoplankton dynamics in the eastern tropical Atlantic, *J. Geophys. Res.*, 102, 12389–12411, 1997.
- Murray, J. W., Barber, R. T., Roman, M. R., Bacon, M. P., and Feely, R. A.: Physical and biological controls on carbon cycling in the equatorial Pacific, *Science*, 266, 58–65, 1994.
- Murtugudde, R. and Busalacchi, A. J.: Interannual variability of the dynamics and thermodynamics of the tropical Indian Ocean, *J. Climate*, 12, 2300–2326, 1999.
- 10 Nagura, M. and McPhaden, M. J.: Wyrтки Jet dynamics: seasonal variability, *J. Geophys. Res.*, 115, C07009, doi:10.1029/2009jc005922, 2010.
- Narvekar, J. and Prasanna Kumar, S.: Upper ocean variability of the equatorial Indian Ocean and its relation to chlorophyll pigment concentration, in: *Proceedings of OceanObs'09: Sustained Ocean Observations and Information for Society (Annex)*, Venice, Italy, 21–25 September 2009, edited by: Hall, J., Harrison, D. E., and Stammer, D., ESA Publication, WPP-306, doi:10.5270, 2010.
- 15 Platt, T., Subba Rao, D. V., and Irwin, B.: Photosynthesis of picoplankton in the oligotrophic Ocean, *Nature*, 301,702–704, 1983.
- 20 Pond, S. and Pickard, G. L.: *Introductory Dynamical Oceanography*, 2nd edn., Pergamon, New York, 379 pp., 1983.
- Prasanna Kumar, S., Ishida, A., Yoneyama, K., Ramesh Kumar, M. R., Kashino, Y., and Mitsudera, H.: Dynamics and thermodynamics of the Indian Ocean warm pool in a high-resolution global general circulation model, *Deep-Sea Res. Pt. II*, 52, 2031–2047, 2005.
- 25 Prasanna Kumar, S., Sardesai, S., and Ramaiah, N.: A decade of physical and biogeochemical measurements in the Northern Indian ocean, in: *Proceedings of OceanObs'09: Sustained Ocean Observations and Information for Society (Annex)*, Venice, Italy, 21–25 September 2009, edited by: Hall, J., Harrison, D. E., and Stammer, D., ESA Publication, WPP-306, doi:10.5270, 2010.
- 30 Qui, Y., Li, L., and Yu, W.: Behavior of the Wyrтки Jet observed with surface drifting buoys and satellite altimeter, *Geophys. Res., Lett.*, 35, L18607,doi:10.1029/2009GL039120, 2009.

Seasonal cycle of biogenic flux in the equatorial Indian Ocean

P. J. Vidya et al.

[Title Page](#)

[Abstract](#)

[Introduction](#)

[Conclusions](#)

[References](#)

[Tables](#)

[Figures](#)

[⏪](#)

[⏩](#)

[◀](#)

[▶](#)

[Back](#)

[Close](#)

[Full Screen / Esc](#)

[Printer-friendly Version](#)

[Interactive Discussion](#)



Ramaswamy, V. and Gaye, B.: Regional variations in the fluxes of foraminifera carbonate, coccolithophorid carbonate and biogenic opal in the northern Indian Ocean, *Deep-Sea Res. Pt. I*, 53, 271–293, 2006.

Rao, R. R., Girish Kumar, M. S., Ravichandran, M., Rao A. R., Gopalakrishna, V. V., and Thadathil, P.: Interannual variability of Kelvin wave propagation in the wave guides of the equatorial Indian Ocean, the coastal Bay of Bengal and the southeastern Arabian Sea during 1993–2006, *Deep-Sea Res. Pt. I*, 57, 1–13, 2010.

Rayner, N. A., Parker, D. E., Horton, E. B., Folland, C. K., Alexander, L. V., Rowell, D. P., Kent, E. C., and Kaplan, A.: Global analyses of sea surface temperature, sea ice, and night marine air temperature since the late nineteenth century, *J. Geophys. Res.*, 108, 4407, doi:10.1029/2002JD002670, 2003.

Reppin, J., Schott, F. A., Fisher, J., and Quadfasel, D.: equatorial currents and transports in the upper central Indian Ocean: Annual cycle and internal variability, *J. Geophys Res.*, 104, 15495–15514, 1999.

Resplandy, L., Vialard, J., Lévy, M., Aumont, O., and Dandonneau, Y.: Seasonal and intraseasonal biogeochemical variability in the thermocline ridge of the southern tropical Indian Ocean, *J. Geophys. Res.*, 114, C07024, doi:10.1029/2008JC005246, 2009.

Reverdin, G.: The upper equatorial Indian Ocean: the multi-year averaged seasonal cycle, *J. Phys. Oceanogr.*, 17, 903–927, 1987.

Reverdin, G. and Luyten, J.: Near-surface meanders in the equatorial Indian Ocean, *J. Phys. Oceanogr.*, 16, 1088–1100, 1986.

Rixen, T., Ittekkot, V., Herunadi, B., Wetzel, P., Maier-Reimer, E., and Gaye-Hakke, B.: ENSO-driven carbon sea saw in the Indo-Pacific, *Geophys. Res. Lett.*, 33, L07606, doi:10.1029/2005GL024965, 2006.

Rixen, T., Ramaswamy, V., Gaye, G., Herunadi, B., Maier-Reimer, E., Bange, H. W., and Ittekkot, V.: Monsoonal and ENSO Impacts on Particle Fluxes and the Biological Pump in the Indian Ocean, *Indian Ocean Biogeochemical Processes and Ecological Variability*, Geophysical Monograph 185, edited by: Wiggert, J. D., Hood, R. R., Naqvi, S. W. A., Brink, K. H., and Smith, S. L., American Geophysical Union, Washington, DC, 365–383, doi:10.1029/2008GM000706, 2009.

Sardessai, S., Suhas Shetye, Maya, M. V., Mangala, K. R., and Prasanna Kumar, S.: Nutrient characteristics of the water masses and their seasonal variability in the eastern equatorial Indian Ocean, *Mar. Environ. Res.*, 70, 272–282, 2010.

Seasonal cycle of biogenic flux in the equatorial Indian Ocean

P. J. Vidya et al.

[Title Page](#)

[Abstract](#)

[Introduction](#)

[Conclusions](#)

[References](#)

[Tables](#)

[Figures](#)

[⏪](#)

[⏩](#)

[◀](#)

[▶](#)

[Back](#)

[Close](#)

[Full Screen / Esc](#)

[Printer-friendly Version](#)

[Interactive Discussion](#)

Sarin, M. M., Krishnaswami, S., Dalai, T. K., Ramaswamy, V., and Ittekkot, V.: Settling fluxes of U- and Th-series nuclides in the Bay of Bengal, results from time-series sediment trap studies, *Deep-Sea Res. Pt. I*, 47, 1961–1985, 2000.

Schiller, A., Godfrey, J. S., McIntosh, P. C., Meyers G., and Fielder, R.: Interannual dynamics and thermodynamics of the Indo-Pacific oceans, *J. Phys. Oceanogr.*, 30, 987–1012, 2000.

Schott, F. and McCreary, J. P.: The monsoon circulation of the Indian Ocean, *Prog. Oceanogr.*, 51, 1–123, 2001.

Schott, F., Dengler, M., and Schoenefeldt, R.: The shallow thermohaline circulation of the Indian Ocean, *Prog. Oceanogr.*, 53, 57–103, 2002.

Shankar, D., Vinayachandran, P. N., and Unnikrishnan, A. S.: The monsoon currents in the north Indian Ocean, *Prog. Oceanogr.*, 52, 63–120, 2002.

Shetye, S. R. and Gouveia, A. D.: Coastal circulation in the North Indian Ocean, in: *The Sea*, edited by: Robinson, A. R. and Brink, K. H., John Wiley & Sons, Inc., New York, 11, 523–556, 1998.

Siegel, D. A. and Deuser, W. G.: Trajectories of sinking particles in the Sargasso Sea: modeling of statistical funnels above deep-ocean sediment traps, *Deep-Sea Res. Pt. I*, 44, 1519–1541, doi:10.1016/S0967-0637(97)00028-9, 1997.

Siegel, D. A. and Franz, B. A.: Century of phytoplankton change, *Nature*, 466, 569–571, 2010.

Siegel, D. A., Iturriaga, R., Bidigare, R. R., Pak, H., Smith, R. C., Dickey, T. D., Marra, J., and Baker, K. S.: Meridional variations of the springtime phytoplankton community in the Sargasso Sea, *J. Mar. Res.*, 48, 379–412, 1990.

Siegel, D. A., Fields, E., and Buesseler, K. O.: A bottom-up view of the biological pump: modeling source funnels above ocean sediment traps, *Deep-Sea Res. Pt. I*, 55, 108–127, doi:10.1016/j.dsr.2007.10.006, 2008.

Stalcup, M. C. and Metcalf, W. G.: Direct measurements of the Atlantic equatorial undercurrent, *J. Mar. Res.*, 24, 44–55, 1966.

Subrahmanyam, R.: A systematic account of the marine plankton diatoms of the Madras coast I, *P. Indian Acad. Sci.*, 24, 85–197, 1946.

Tomas Carmelo, R.: *Identifying Marine Phytoplankton*, Academic, UK, 29–549, 1997.

Tsai, P. T. H., O'Brien, J. J., and Luther, M. E.: The 26-day oscillation observed in the Satellite Sea surface temperature measurements in the equatorial western Indian Ocean, *J. Geophys. Res.*, 97, 9605–9618, 1992.

Seasonal cycle of biogenic flux in the equatorial Indian Ocean

P. J. Vidya et al.

[Title Page](#)

[Abstract](#)

[Introduction](#)

[Conclusions](#)

[References](#)

[Tables](#)

[Figures](#)

[⏪](#)

[⏩](#)

[◀](#)

[▶](#)

[Back](#)

[Close](#)

[Full Screen / Esc](#)

[Printer-friendly Version](#)

[Interactive Discussion](#)

UNESCO: Protocols for the Joint Global Ocean Flux Study (JGOFS), Manual and Guide, 97–128, 1994.

Unger, D. and Jennerjahn, T.: Impact of regional Indian Ocean characteristics on the biogeochemical variability of settling particles, *Geoph. Monog. Series*, 185, 257–280, doi:10.1029/2008GM000703, 2009.

Unger, D., Ittekkot, V., Schafer, P., Tiemann J., and Reschke, S.: Seasonality and interannual variability of particle fluxes to the deep Bay of Bengal: influence of riverine input and oceanographic processes, *Deep-Sea Res. Pt. II*, 50, 897–923, 2003.

Unger, D., Schäfer, P., Ittekkot, V., and Gaye, B.: Nitrogen isotopic composition of sinking particles from the Southern Bay of Bengal: evidence for variable nitrogen sources, *Deep-Sea Res. Pt. I*, 53, 1658–1676, 2006.

Voss, R. and Sausen, R.: Techniques for asynchronous and periodically synchronous coupling of atmosphere and ocean models, Part II: impact of variability, *Clim. Dynam.*, 12, 605–614, 1996.

Voiturie, B. and Herbrand, A.: Primary production in the tropical Atlantic Ocean mapped from the oxygen values of Equalant 1 and 2 (1963), *B. Mar. Sci.*, 31, 853–863, 1981.

Waniek, J. J., Schulz-Bull, D. E., Blanz, T., Prien R., D., Oschlies, A., and Muller, T. J.: Interannual variability of deep water particle flux in relation to production and lateral sources in the northeast Atlantic, *Deep-Sea Res. Pt. I*, 52, 33–50, 2005.

Wefer, G. and Fischer, G.: Seasonal pattern of vertical particle flux in the equatorial and coastal upwelling areas of the eastern Atlantic, *Deep-Sea Res. Pt. I*, 40, 1613–1645, 1993.

Wiggert, J. D., Murtugudde, R. G., and Christian, J. R.: Annual ecosystem variability in the tropical Indian Ocean: results of a coupled bio-physical ocean general circulation model, *Deep-Sea Res. Pt. II*, 53, 644–676, 2006.

Wiggert, J. D., Vialard, J., and Behrenfeld, M. J.: Basin-wide modification of dynamical and biogeochemical processes by the positive phase of the Indian Ocean dipole during the SeaWiFS era, *Indian Ocean Biogeochemical Processes and Ecological Variability*, *Geophysical Monograph* 185, edited by: Wiggert, J. D., Hood, R. R., Naqvi, S. W. A., Brink, K. H., and Smith, S. L, American Geophysical Union, Washington, DC, 385–407, doi:10.1029/2008GM000776, 2009.

Wyrтки, K.: An equatorial jet in the Indian Ocean, *Science*, 181, 262–264, 1973.

Table 1. Phytoplankton composition and numerical abundance (cells L⁻¹) at selected stations in the vicinity of SBBT (5° N; 83° E) and EIOT (2.5° N; 77° E) during August 2006.

SK 227 – 1–30 August 2006 Depths (m)	5° N, 83° E						2.5° N, 77° E									
	0	10	20	40	60	80	100	120	0	10	20	40	60	80	100	120
Diatoms (cells L⁻¹)																
Centric	-	-	-	-	-	-	-	-	-	-	-	-	-	-	-	-
<i>Biddulphia</i> sp.	-	-	-	-	-	-	-	96	-	-	-	-	-	-	-	-
<i>Chaetoceros danicus</i>	-	-	-	-	-	160	-	-	-	-	-	-	-	-	-	-
<i>Chaetoceros didymus</i>	-	-	-	336	-	160	-	-	-	-	-	-	-	-	-	-
<i>Chaetoceros</i> sp.	-	-	264	-	-	-	-	-	-	-	-	-	-	-	-	-
<i>Coscinodiscus granii</i>	-	-	88	-	-	-	-	-	-	-	-	-	-	-	-	-
<i>Coscinodiscus perforatus</i>	-	-	-	-	-	-	-	-	-	-	56	56	-	-	-	-
<i>Coscinodiscus</i> sp.	-	-	-	-	-	-	-	-	-	-	56	-	-	-	-	-
<i>Guinardia flaccida</i>	-	-	88	-	-	-	-	-	-	-	-	-	-	-	-	-
<i>Leptocylindrus danicus</i>	-	-	-	112	-	-	-	-	240	96	-	-	-	96	-	-
<i>Rhizosolenia curvata</i>	-	-	88	-	-	-	-	-	-	-	-	-	-	-	-	-
<i>Rhizosolenia imbricata</i>	-	-	240	-	-	-	-	-	-	-	-	-	-	-	-	-
<i>Rhizosolenia setigera</i>	-	-	-	336	-	-	-	-	-	-	-	-	-	-	-	-
<i>Rhizosolenia styliformis</i>	168	240	88	672	240	-	-	-	-	-	-	-	-	-	-	-
Pennate	-	-	-	-	-	-	-	-	-	-	-	-	-	-	-	-
<i>Amphora</i> sp.	-	-	-	224	-	-	-	-	-	-	-	-	-	-	-	-
<i>Pseudonitzschia turgidula</i>	-	-	-	-	-	-	-	768	-	-	-	-	-	-	-	-
<i>Navicula membranaceae</i>	-	160	-	-	-	-	-	-	-	-	-	-	-	-	-	-
<i>Navicula</i> sp.	-	-	-	224	-	-	-	-	-	-	-	-	-	-	-	-
<i>Nitzschia delicatissima</i>	-	-	-	336	80	-	-	-	-	-	-	-	-	-	-	-
<i>Nitzschia longissima</i>	-	-	-	-	80	-	-	-	-	-	-	-	-	-	-	-
<i>Nitzschia</i> sp.	-	-	-	-	-	-	-	-	-	56	-	56	-	-	-	-
<i>Synedra</i> sp.	-	-	-	-	-	-	-	-	48	-	112	-	-	-	-	-
<i>Thalassiothrix longissima</i>	-	-	-	80	-	-	-	-	96	-	-	-	-	-	-	-
Dinoflagellates (cells L⁻¹)	-	-	-	-	-	-	-	-	-	-	-	-	-	-	-	-
<i>Alexandrium</i> sp.	-	-	-	-	80	-	-	-	-	-	-	-	-	-	-	-
<i>Ceratium trichoceros</i>	-	-	-	-	-	-	-	-	-	-	56	-	-	-	-	-
<i>Ceratium</i> sp.	-	-	-	-	-	-	84	-	-	-	-	-	-	-	-	-
<i>Gonyaulax</i> sp.	84	-	-	-	-	-	-	-	-	-	-	-	-	-	-	-
<i>Gymnodinium</i> sp.	-	160	-	-	-	-	-	-	-	-	-	-	-	-	-	-
<i>Ornithoceros</i> sp.	-	-	-	112	-	-	-	-	-	-	-	-	-	-	-	-
<i>Phalacroma circumsutum</i>	-	-	-	-	-	-	-	40	-	-	-	-	-	-	-	-
<i>Peridinium</i> sp.	-	-	88	-	-	-	-	-	-	-	-	-	-	-	-	-
<i>Polykrikos</i> sp.	-	-	-	-	80	-	-	-	-	-	-	-	-	-	-	-
<i>Prorocentrum micans</i>	-	-	-	-	160	-	-	-	-	-	-	-	-	-	-	-
<i>Prorocentrum</i> sp.	-	80	-	-	-	-	-	-	-	-	-	-	-	-	-	-
<i>Protoperdinium</i> sp.	-	-	-	-	80	-	-	-	-	-	-	-	-	-	-	-
<i>Pyrophacus</i> sp.	-	-	-	-	80	-	-	-	-	-	56	-	-	-	-	-
<i>Dinoflagellate cyst</i>	-	-	-	-	-	-	-	-	96	-	-	224	-	128	256	-
Unidentified Phytoplanktons	80	224	80	1176	-	-	-	-	-	-	-	-	-	-	-	-
Total (cells L⁻¹)	252	960	704	2576	1040	320	1260	864	280	336	56	280	336	96	128	256

Seasonal cycle of biogenic flux in the equatorial Indian Ocean

P. J. Vidya et al.

[Title Page](#)

[Abstract](#)

[Introduction](#)

[Conclusions](#)

[References](#)

[Tables](#)

[Figures](#)

[⏪](#)

[⏩](#)

[◀](#)

[▶](#)

[Back](#)

[Close](#)

[Full Screen / Esc](#)

[Printer-friendly Version](#)

[Interactive Discussion](#)



Table 2. Comparison of primary productivity, biogenic flux, organic carbon flux and export at SBBT and EIOT with that of equatorial Pacific and equatorial Atlantic oceans. Primary productivity is integrated within the euphotic zone, the biogenic flux and carbon flux are measured at a nominal depth of 1000. The carbon export (%) was calculated using the formula $\text{Export (\%)} = [\text{C}_{\text{org}} \text{ Flux (mgm}^{-2}\text{d}^{-1}) / \text{Primary Production (mgCm}^{-2}\text{d}^{-1})] \times 100$ given by Honjo et al. (1995).

Ocean basin		Primary productivity ($\text{mgCm}^{-2}\text{d}^{-1}$)	Biogenic flux ($\text{mgm}^{-2}\text{d}^{-1}$)	Carbon flux ($\text{mgm}^{-2}\text{d}^{-1}$)	Export (%)
equatorial Indian Ocean	EIOT (2.5° N)	288.2	37.4	5.7	2.0
	SBBT (5° N)	353.6	160.9	12	3.4
equatorial Pacific ^a (5° N)		500.0	88.6	4.5	0.9
equatorial Atlantic (1.5° N)		500.0 ^b	216.1 ^c	30.4 ^c	6.0

^a Honjo et al., 1995; ^b Voituriez and Herbland, 1981; ^c Wefer and Fisher, 1993

Seasonal cycle of biogenic flux in the equatorial Indian Ocean

P. J. Vidya et al.

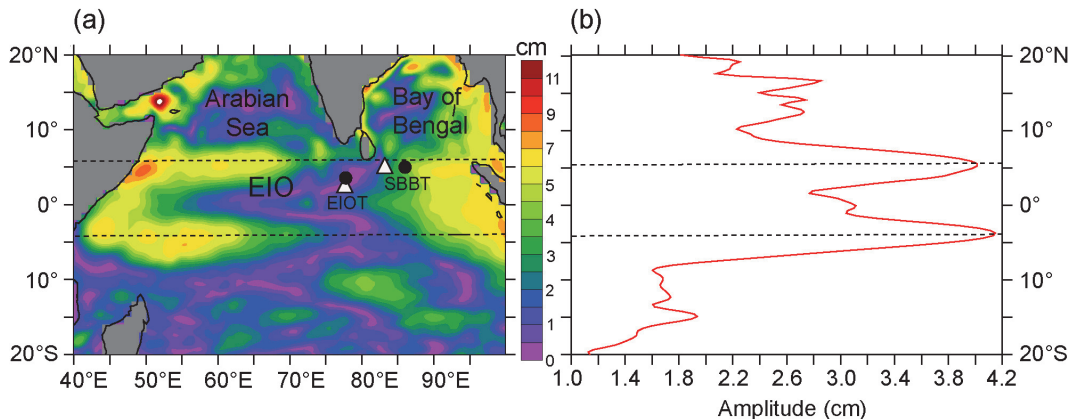


Fig. 1. (a) Spatial distribution of semi-annual amplitude of SSHA (cm) and (b) zonal distribution of meridionally averaged semi-annual amplitude of SSHA (cm) in the Indian Ocean. Broken line defines the boundary of equatorial Indian Ocean (EIO) (see text for details). Filled black circles represent the sediment trap location SBBT and EIO and filled white triangles represent the in-situ observation on board ORV Sagar Kanya during August 2006.

Title Page

Abstract

Introduction

Conclusions

References

Tables

Figures

◀

▶

◀

▶

Back

Close

Full Screen / Esc

Printer-friendly Version

Interactive Discussion

Seasonal cycle of biogenic flux in the equatorial Indian Ocean

P. J. Vidya et al.

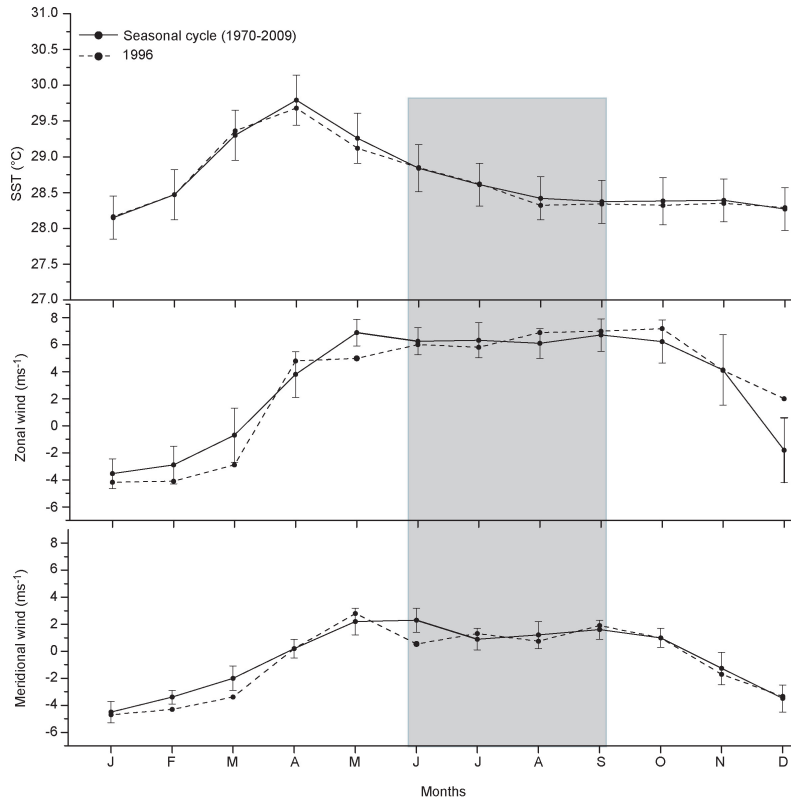


Fig. 2. Climatological monthly mean during the period 1970–2009 (thick line), and monthly mean of 1996 (dotted line) of SST (upper panel), zonal wind (middle panel) and meridional wind (bottom panel). Shading represents the summer monsoon period (June–September) and vertical lines are one standard deviation.

Seasonal cycle of biogenic flux in the equatorial Indian Ocean

P. J. Vidya et al.

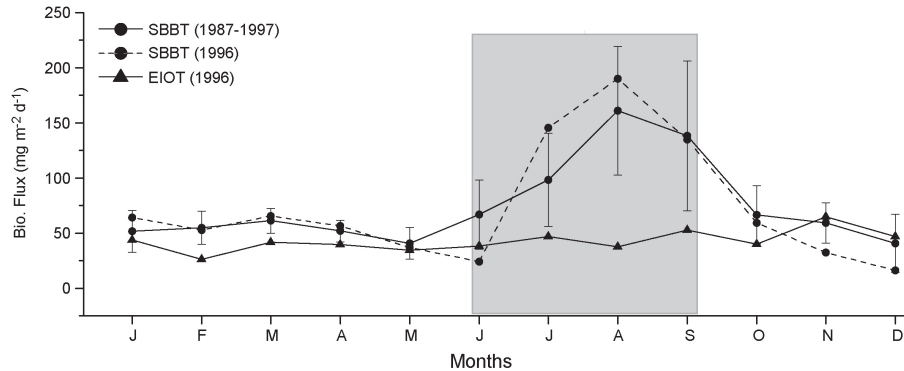


Fig. 3. Monthly mean climatology (1987–1997) of biogenic flux ($\text{mg m}^{-2} \text{d}^{-1}$) at SBBT (solid line with filled circle) and monthly mean biogenic flux for the year 1996 at SBBT (broken line with filled circles) and EIOT (filled triangle). Shading represents the summer monsoon period (June–September) and vertical lines are one standard deviation.

Title Page

Abstract

Introduction

Conclusions

References

Tables

Figures

◀

▶

◀

▶

Back

Close

Full Screen / Esc

Printer-friendly Version

Interactive Discussion

Seasonal cycle of biogenic flux in the equatorial Indian Ocean

P. J. Vidya et al.

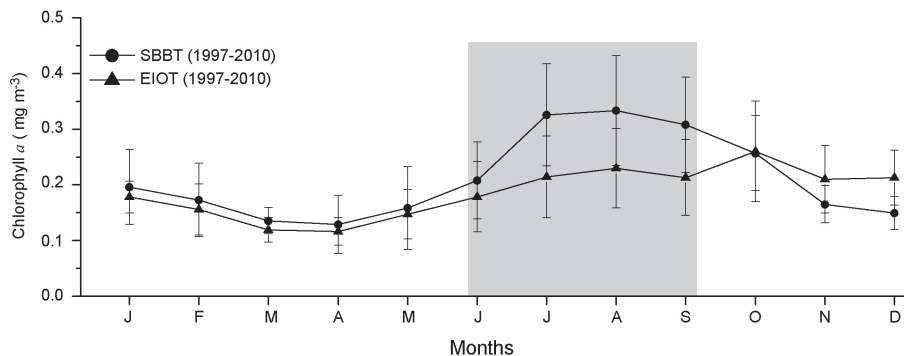


Fig. 4. Monthly mean climatology (1997–2010) of satellite derived chlorophyll pigment concentration at SBBT (filled circle) and EIOT (filled triangle). Shading represents the summer monsoon period (June–September) and vertical lines are one standard deviation.

[Title Page](#)
[Abstract](#)
[Introduction](#)
[Conclusions](#)
[References](#)
[Tables](#)
[Figures](#)
[⏪](#)
[⏩](#)
[◀](#)
[▶](#)
[Back](#)
[Close](#)
[Full Screen / Esc](#)
[Printer-friendly Version](#)
[Interactive Discussion](#)

Seasonal cycle of biogenic flux in the equatorial Indian Ocean

P. J. Vidya et al.

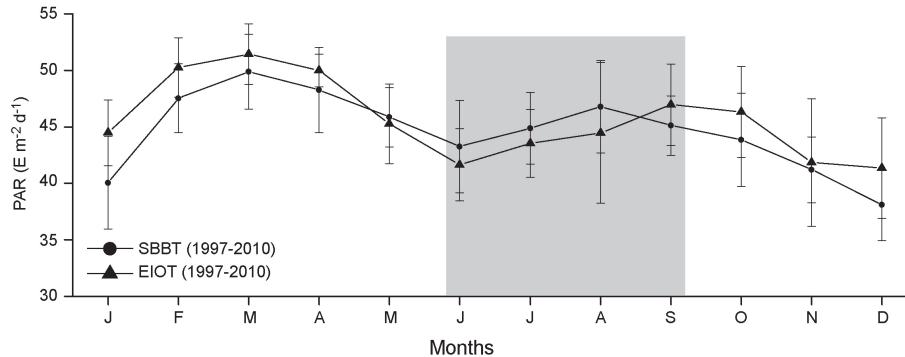


Fig. 5. Monthly mean climatography (1997–2010) of photosynthetically active radiation (PAR) at SBBT (filled circle) and EIOT (filled triangle). Shading represents the summer monsoon period (June–September) and vertical lines are one standard deviation.

Title Page

Abstract

Introduction

Conclusions

References

Tables

Figures

◀

▶

◀

▶

Back

Close

Full Screen / Esc

Printer-friendly Version

Interactive Discussion

Seasonal cycle of biogenic flux in the equatorial Indian Ocean

P. J. Vidya et al.

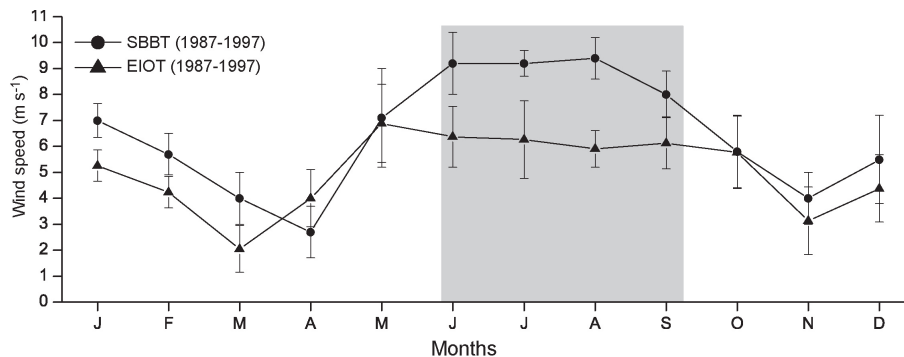


Fig. 6. Monthly mean climatology (1987–1997) of ECMWF wind speed (m s^{-1}) at SBBT (filled circle) and EIoT (filled triangle). Shading represents the summer monsoon period (June–September) and vertical lines are one standard deviation.

[Title Page](#)[Abstract](#)[Introduction](#)[Conclusions](#)[References](#)[Tables](#)[Figures](#)[⏪](#)[⏩](#)[◀](#)[▶](#)[Back](#)[Close](#)[Full Screen / Esc](#)[Printer-friendly Version](#)[Interactive Discussion](#)

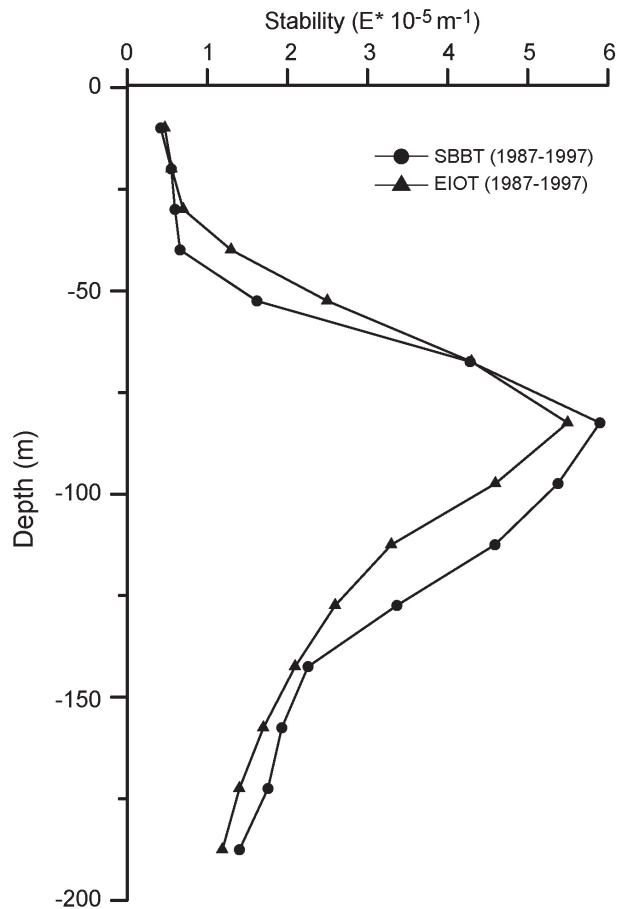


Fig. 7. Monthly mean climatology (1987–1997) of static stability of the water column (m^{-1}) at SBBT (filled circle) and EIOT (filled triangle) (see text for details) during August.

Seasonal cycle of biogenic flux in the equatorial Indian Ocean

P. J. Vidya et al.

[Title Page](#)

[Abstract](#) | [Introduction](#)

[Conclusions](#) | [References](#)

[Tables](#) | [Figures](#)

[◀](#) | [▶](#)

[◀](#) | [▶](#)

[Back](#) | [Close](#)

[Full Screen / Esc](#)

[Printer-friendly Version](#)

[Interactive Discussion](#)



Seasonal cycle of biogenic flux in the equatorial Indian Ocean

P. J. Vidya et al.

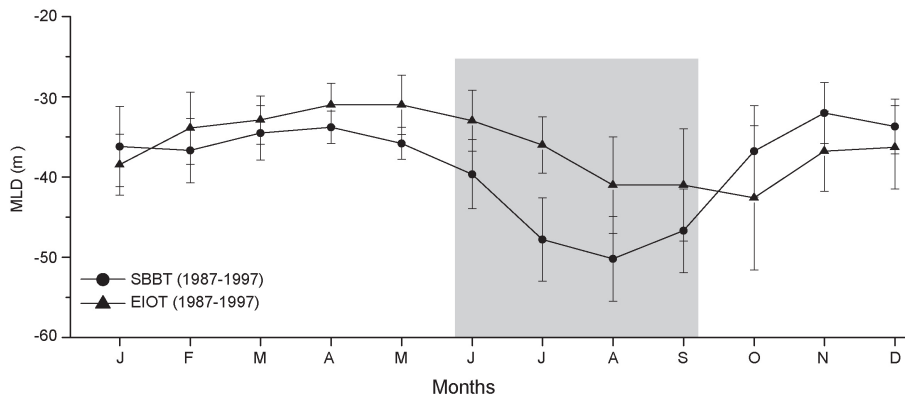


Fig. 8. Monthly mean climatology (1987–1997) of mixed layer depth (MLD), at SBBT (filled circle) and EIoT (filled triangle). Shading represents the summer monsoon period (June–September) and vertical lines are one standard deviation.

[Title Page](#)[Abstract](#)[Introduction](#)[Conclusions](#)[References](#)[Tables](#)[Figures](#)[⏪](#)[⏩](#)[◀](#)[▶](#)[Back](#)[Close](#)[Full Screen / Esc](#)[Printer-friendly Version](#)[Interactive Discussion](#)

Seasonal cycle of biogenic flux in the equatorial Indian Ocean

P. J. Vidya et al.

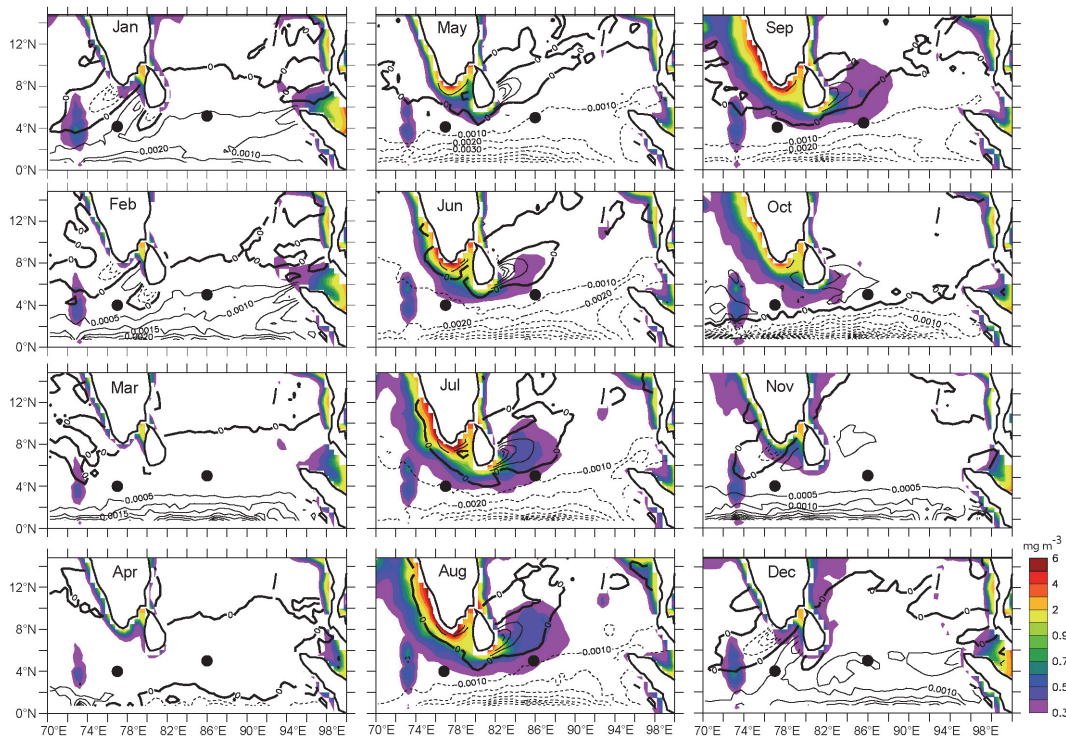


Fig. 9. Spatial distribution of monthly mean climatology (1997–2010) of the chlorophyll $\geq 0.3 \text{ mg m}^{-3}$ (shading) overlaid with Ekman-pumping velocity (contour lines) for January to December. Solid (dashed) lines are for positive (negative) values and thick solid line is for zero Ekman-pumping velocity. Filled circles denote the location of SBBT and EIOT.

[Title Page](#)
[Abstract](#)
[Introduction](#)
[Conclusions](#)
[References](#)
[Tables](#)
[Figures](#)
[Back](#)
[Close](#)
[Full Screen / Esc](#)
[Printer-friendly Version](#)
[Interactive Discussion](#)

Seasonal cycle of biogenic flux in the equatorial Indian Ocean

P. J. Vidya et al.

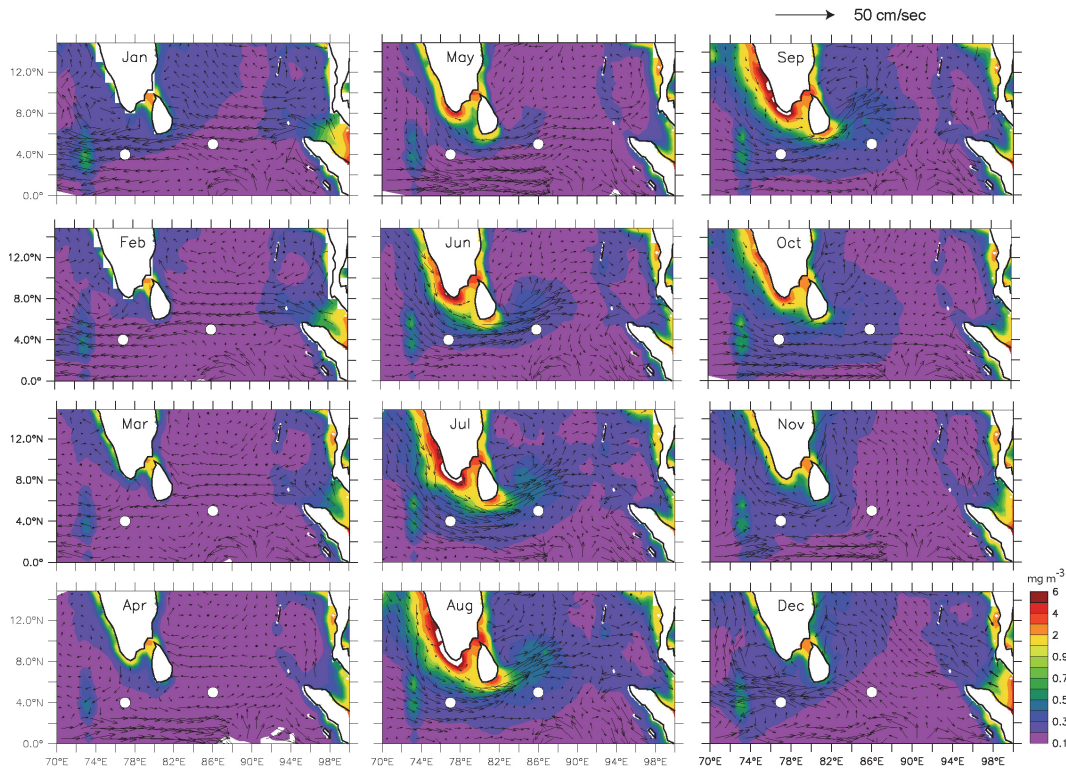


Fig. 10. Monthly mean climatology (1997–2010) of chlorophyll pigment concentration (mg m^{-3}) (shading) overlaid with OSCAR current (arrows), white circles represent location of SBBT and EIOT.

[Title Page](#)
[Abstract](#)
[Introduction](#)
[Conclusions](#)
[References](#)
[Tables](#)
[Figures](#)
[Back](#)
[Close](#)
[Full Screen / Esc](#)
[Printer-friendly Version](#)
[Interactive Discussion](#)

Seasonal cycle of biogenic flux in the equatorial Indian Ocean

P. J. Vidya et al.

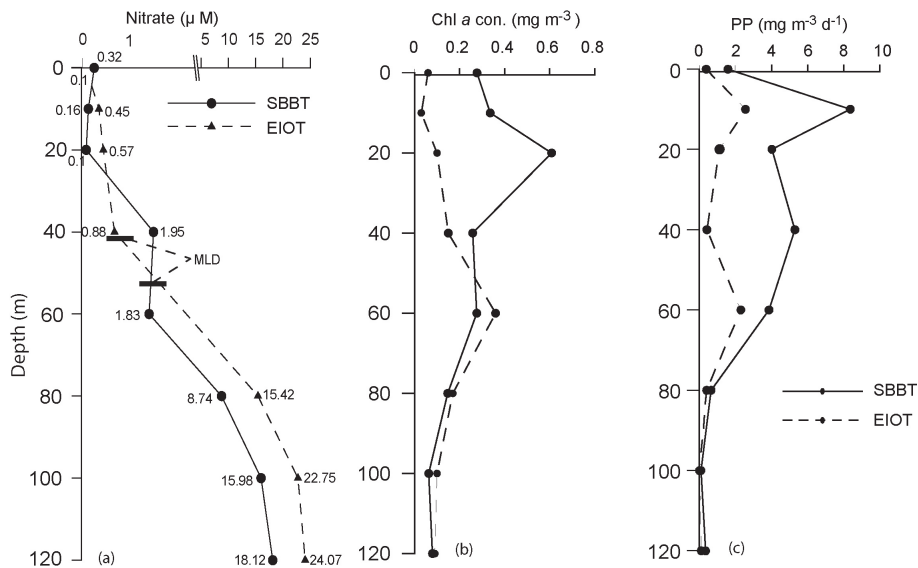


Fig. 11. Vertical profiles of (a) nitrate (μM) (thick black line cutting across the profiles represent the mixed layer depth), (b) chlorophyll *a* (mg m^{-3}) and (c) primary production ($\text{mg C m}^{-3} \text{ d}^{-1}$) in the vicinity of SBBT (solid line) and EIOT (broken line) during August 2006. In Fig. 11a., the thick line cutting across the profiles represent the mixed layer depth.

Title Page

Abstract Introduction

Conclusions References

Tables Figures

◀ ▶

◀ ▶

Back Close

Full Screen / Esc

Printer-friendly Version

Interactive Discussion



Seasonal cycle of biogenic flux in the equatorial Indian Ocean

P. J. Vidya et al.

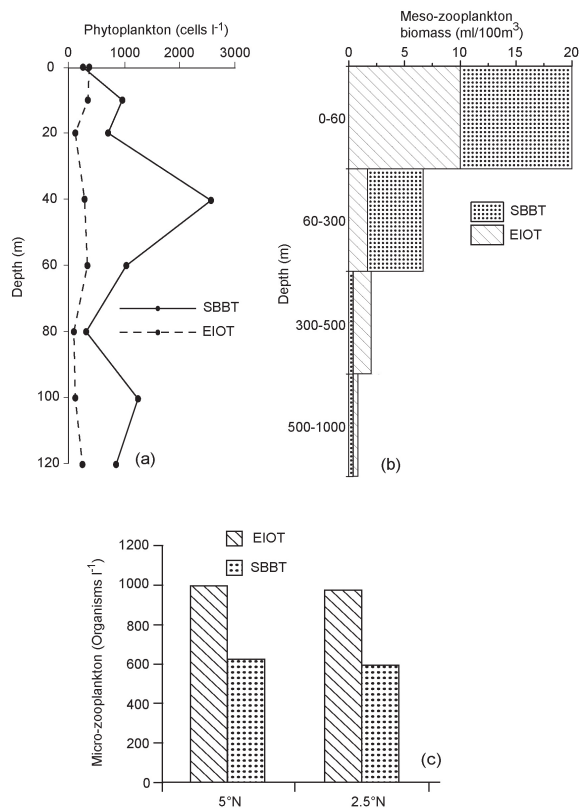


Fig. 12. Vertical profiles of **(a)** phytoplankton abundance (cells l^{-1}) in the vicinity of SBBT (solid line) and EIOT (broken line) **(b)** vertically stratified meso-zooplankton biomass in the vicinity of SBBT (dots) and EIOT (hatches) and **(c)** Microzooplankton (organisms l^{-1}) at selected stations along SBBT (dots) and EIOT (hatches) during August 2006.

Seasonal cycle of biogenic flux in the equatorial Indian Ocean

P. J. Vidya et al.

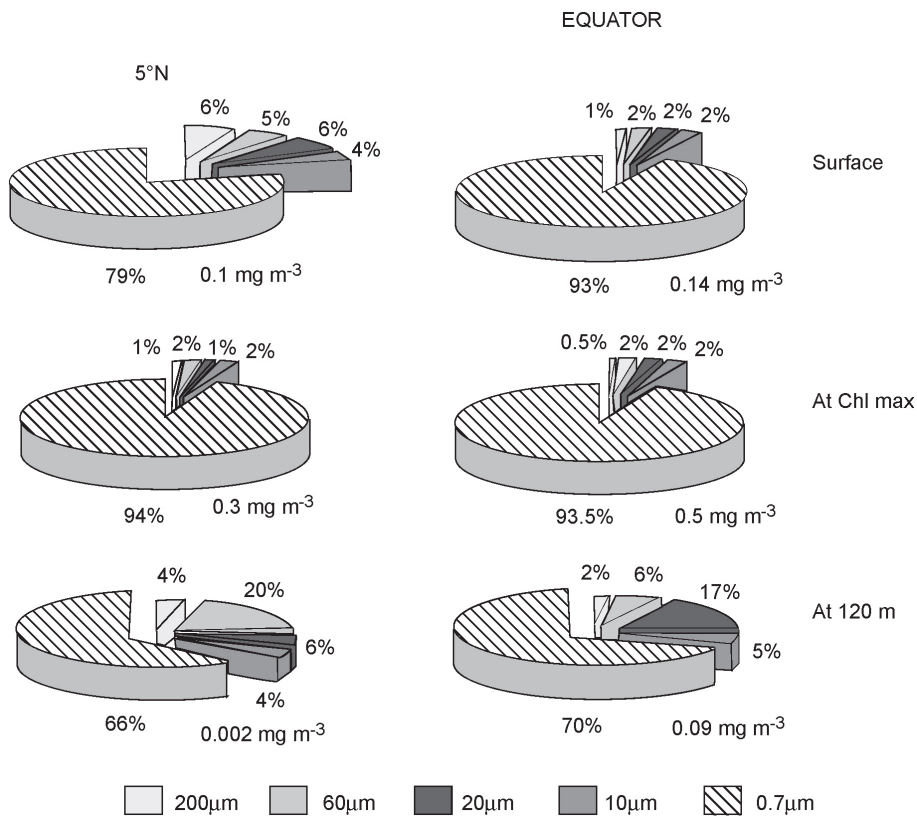


Fig. 13. Size fractionated phytoplankton biomass (mg Chl *a* m⁻³) during August 2006 at 5° N (left panels) and Equator (right panels) along 77° E from surface (top panels), chlorophyll maximum (middle panels) and at 120 m (bottom panels).

Title Page

Abstract Introduction

Conclusions References

Tables Figures

◀ ▶

◀ ▶

Back Close

Full Screen / Esc

Printer-friendly Version

Interactive Discussion



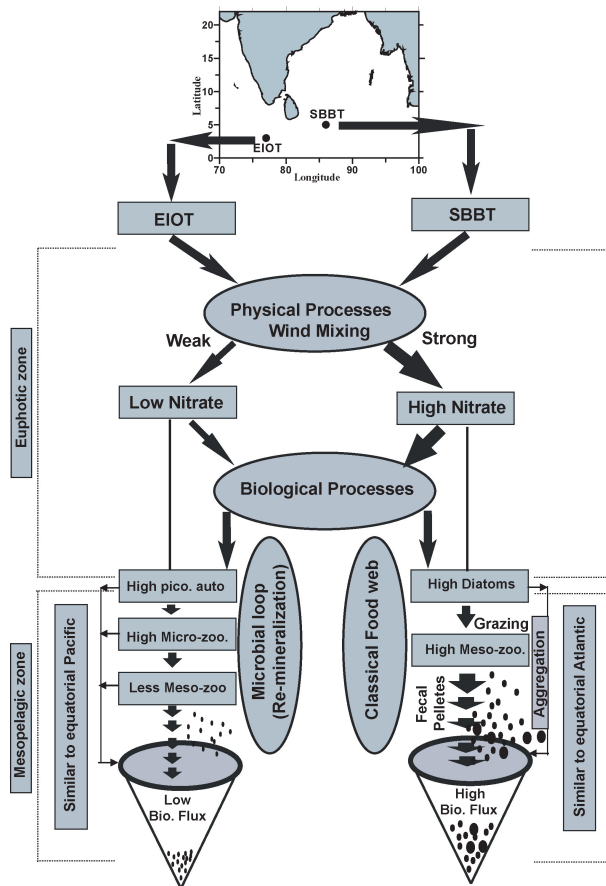


Fig. 14. Schematic picture summarizing the physical and biological processes starting from production of organic carbon in the upper ocean to its export into the deep ocean as captured by the sediment trap at SBBT and EIoT.